Received: 25 March 2022 | Revised: 18 November 2022 | Accepted: 9 December 2022

DOI: 10.1111/gcb.16562

Global Change Biology WILEY

RESEARCH ARTICLE

Future area expansion outweighs increasing drought risk for soybean in Europe

Claas Nendel[1,2,3] | Moritz Reckling[1,4] | Philippe Debaeke[5] | Susanne Schulz[1] | Michael Berg-Mohnicke[1] | Julie Constantin[5] | Stefan Fronzek[6] | Munir Hoffmann[7] | Snežana Jakšić[8] | Kurt-Christian Kersebaum[1,3,9] | Agnieszka Klimek-Kopyra[10] | Hélène Raynal[5] | Céline Schoving[5,11] | Tommaso Stella[1] | Rafael Battisti[12]

[1]Leibniz Centre for Agricultural Landscape Research (ZALF), Müncheberg, Germany

[2]Institute of Biochemistry and Biology, University of Potsdam, Potsdam, Germany

[3]Global Change Research Institute, The Czech Academy of Sciences, Brno, Czech Republic

[4]Department of Crop Production Ecology, Swedish University of Agricultural Sciences, Uppsala, Sweden

[5]Université de Toulouse, INRAE, UMR AGIR, Castanet-Tolosan, France

[6]Finnish Environment Institute (SYKE), Helsinki, Finland

[7]Agvolution GmbH, Göttingen, Germany

[8]Institute of Field and Vegetable Crops, Novi Sad, Republic of Serbia

[9]Tropical Plant Production and Agricultural Systems Modelling, Georg-August-Universität Göttingen, Göttingen, Germany

[10]Faculty of Agriculture and Economics, University of Agriculture in Krakow, Kraków, Poland

[11]Terres Inovia, Baziege, France

[12]School of Agronomy, Federal University Goiás, Goiânia, Brazil

Correspondence
Claas Nendel, Leibniz Centre for Agricultural Landscape Research (ZALF), Eberswalder Straße 84, 15374 Müncheberg, Germany.
Email: claas.nendel@zalf.de

Funding information
Federal Ministry of Education and Research (BMBF), Germany, Grant/Award Number: 01DR17011A; Academy of Finland, Grant/Award Number: 330915; Ministry of Education, Youth and Sports of the Czech Republic, Grant/Award Number: CZ.02.1.01/0.0/0.0/16_019/0 00797

Abstract

The European Union is highly dependent on soybean imports from overseas to meet its protein demands. Individual Member States have been quick to declare self-sufficiency targets for plant-based proteins, but detailed strategies are still lacking. Rising global temperatures have painted an image of a bright future for soybean production in Europe, but emerging climatic risks such as drought have so far not been included in any of those outlooks. Here, we present simulations of future soybean production and the most prominent risk factors across Europe using an ensemble of climate and soybean growth models. Projections suggest a substantial increase in potential soybean production area and productivity in Central Europe, while southern European production would become increasingly dependent on supplementary irrigation. Average productivity would rise by 8.3% (RCP 4.5) to 8.7% (RCP 8.5) as a result of improved growing conditions (plant physiology benefiting from rising temperature and CO_2 levels) and farmers adapting to them by using cultivars with longer phenological cycles. Suitable production area would rise by 31.4% (RCP 4.5) to 37.7% (RCP

8.5) by the mid-century, contributing considerably more than productivity increase to the production potential for closing the protein gap in Europe. While wet conditions at harvest and incidental cold spells are the current key challenges for extending soybean production, the models and climate data analysis anticipate that drought and heat will become the dominant limitations in the future. Breeding for heat-tolerant and water-efficient genotypes is needed to further improve soybean adaptation to changing climatic conditions.

KEYWORDS
genotypes, legumes, maturity groups, protein crops, protein transition, resilience

1 | INTRODUCTION

The European Union (EU) estimated its annual demand for plant proteins at 27 million tonnes, of which 93% was required for animal production, with only 0.15% for human consumption (European_Commission, 2018). Each year, the EU imports around 17 million tonnes of crude proteins, including 12 million tonnes of soybean proteins, most of which come from Brazil, Argentina and the United States (Eurostat, 2021). Environmental and social concerns have led the European Commission to issue a plant protein strategy (European_Commission, 2018) to reduce Europe's dependency on protein imported from overseas. One declared objective of this strategy is to make cultivation of soybean and other protein crops in Europe more profitable and competitive. This also reflects the European Commission's awareness of the need to reduce meat-based diets as an important cornerstone in the battle against climate change, health problems among Europeans (Willett et al., 2019) and deforestation in the Amazon Region (Karlsson et al., 2021). The Green Deal (European_Commission, 2019) should support this strategy by highlighting soybean and other legumes as key constituents in the diversification strategy towards more sustainable farming. Promoting vegetable proteins in line with this goal requires greater production of legume crops. Among these, soybean exhibits the largest potential, on account of its high seed protein concentration of 39%–48% on a dry matter basis (e.g. Karges et al., 2022), the large temperature range in which it can be cultivated, and the wealth of existing agronomic knowledge from other continents. When tapping the still underused potential of soybean for human consumption (Siebert & Tränkner-Benslimane, 2020), European producers have a competitive advantage since soybean production on the continent avoids genetically modified varieties (Eriksson et al., 2019), which the majority of European consumers see as a benefit.

In Europe, soybean still plays a minor role in agriculture. Only 2.7 million tonnes of soybean were produced in the EU in 2020/2021, while non-EU European countries produced another 8.4 million tonnes (Eurostat, 2021; FAOSTAT, 2019). The few areas in Europe where soybean is grown are concentrated between 45°N and 50°N latitude, with the largest production in 2019 in eastern Europe (Ukraine, 3.7 million tonnes; Serbia, 0.7 million tonnes; Romania 0.4 million tonnes) and in the northern Mediterranean (Italy, 1.0 million tonnes; France, 0.4 million tonnes) (FAOSTAT, 2019). Based on agronomical knowledge, the general impression of climatic restrictions to soybean cultivation in Europe is as follows: to the east—towards a more continental climate—frequent drought and the risk of early-season cold shocks limit production, while a lower temperature regime and the risk of autumn rains that can hamper harvests both restrict soybean production further north. Insufficient soil water availability is the major constraint to production in the south, while heat stress has not yet led any to notable production risk. Climate change is expected to alter this picture through two different mechanisms: First, farmers' need to adapt production systems to the changing climate, which is likely to result in strong demand for diversifying their crop portfolio as a hedging strategy to mitigate the increasing risk of yield losses and in reviving long-known ecological principles of maintaining soil and crop health (Hufnagel et al., 2020). Profitable legume crops, such as soybean, are surely among the best options for this purpose (Reckling et al., 2020). Second, the projected increase in temperature in Europe will move the area suitable for soybean cultivation northwards (Karges et al., 2022), potentially expanding this area, while allowing for higher-yielding varieties in current soybean production areas (Coleman et al., 2021; Toleikiene et al., 2021). At the same time, increases in temperature and atmospheric CO_2 levels have a positive impact on physiological processes in the plant, allowing for more efficient photosynthesis and water use, and consequently higher productivity (Ainsworth et al., 2002; Kothari et al., 2022; Tacarindua et al., 2013).

Economically viable soybean cultivation requires environmental conditions that suit the crop in terms of day length, temperature and rainfall or available irrigation water. Soybean requires a sufficient number of warm days to mature. Karges et al. (2022) reported that 969–1036 Growing Degree Days above a base temperature of 10°C were sufficient for a site in Central Europe. The temperature below which soybean growth is significantly hampered varies considerably from variety to variety, and there is no detailed analysis on soybean base temperature for Europe. A base temperature of 10°C seems to be an accepted representative value among soybean agronomists (Avila et al., 2013; Hatfield & Egli, 1974; compare also Sinclair et al., 2005). A similar uncertainty exists for temperatures critical for flower abscission ('blossom drop'; Kurosaki & Yumoto, 2003) and

seed cracking (Yamaguchi et al., 2014), a common soybean response to cold temperatures around flowering, with negative consequences for seed yields. Threshold values for blossom drop and seed cracking were reported between 10 and 13°C (Kurosaki & Yumoto, 2003; Ohnishi et al., 2010; Staniak et al., 2021; Yamaguchi et al., 2014). While cold snaps with temperatures below these thresholds sometimes occur in the early soybean growing season (Żarski et al., 2019), late frost is—to our knowledge—not a serious problem, as farmers sow relatively late in the season to minimise this risk.

Soybean photosensitivity is genetically controlled by multiple loci, known as the E series (Jiang et al., 2014; Kurasch et al., 2017). Mutations result in photoperiod insensitivity, and different combinations of photoperiod-insensitive alleles affect the rate of development towards physiological maturity (Jia et al., 2014; Tsubokura et al., 2014). Kurasch et al. (2017) described how photoperiod influences the development rate towards flowering and maturity of soybean, and demonstrated the interaction of photosensitivity and temperature for a range of varieties. Photoperiod-insensitive cultivars seem to be more strongly influenced by temperature, with higher temperatures resulting in earlier flowering (Kurasch et al., 2017; Sun et al., 2011). Breeding has resulted in a large range of varieties suitable for day length and temperature zones that range from southern Sweden into the tropics, and a widely accepted key initially classified them into nine maturity groups (MG) 0–VIII (US Regional Soybean Laboratory, 1946, 1953). Later breeding efforts for long-day suitability gradually added three more groups at the lower end (0000–00: Jia et al., 2014). Even though this day length×temperature range covered by the MGs already allows a broad adaptation across Europe, the early MGs—especially 0000—currently produce significantly lower yields (Ortel et al., 2020) and are, therefore, not very attractive. Season length, as a combination of both factors, is, therefore, still a major constraint for growing soybean in northern latitudes (Yang et al., 2019).

Sufficient water supply is needed at the time of germination and flowering (Mandić et al., 2017). In regions where rainfall is not always available as this water supply, production of soybean is at risk of yield failures due to drought in critical periods (Zipper et al., 2016). Where sufficient water is available in water bodies, irrigation is used to mitigate this risk. Current breeding efforts have concentrated on developing more drought-tolerant varieties as well as on weed-suppressing traits (Klaiss et al., 2020), especially for organic production systems. Rainfall during the later phase of the season, however, can have negative effects on the production process. Since soybean will be in the field until autumn in the northern parts of Europe, the risk of higher rainfall rates increases towards the harvest period. Soybean pods are fragile, and repeated cycles of drying and wetting increase pod shattering and loss of seeds (Đorđević et al., 2021). From the technological perspective, a wet canopy impedes the harvesting process because combine harvesters may clog, and subsequent drying of the seeds may be necessary, which is expensive. In addition, wet soils may prevent heavy combine harvesters from traversing fields.

High temperatures affect soybean growth and yield formation in various ways (Nahar et al., 2016). Most importantly, high temperatures increase the abscission of flowers and pods and reduce pollen viability and stigma receptivity (Boote et al., 2005; Koti et al., 2007; Puteh et al., 2013). Furthermore, the general exceedance of the optimum temperature range for photosynthesis—while respiration still responds positively due to its higher temperature optimum—leads to a reduced assimilate balance, and a negative overall growth response (Boote et al., 2005). The critical temperatures above which physiological processes in soybean are seriously affected are wide-ranging (Nahar et al., 2016). However, first heat-related yield penalties seem to manifest already at temperatures above 30°C (Egli & Wardlaw, 1980; Gibson & Mullen, 1996; Schlenker & Roberts, 2009). Irrigation does not only mitigate drought but also heat stress, because a transpiring soybean crop cools down its canopy by up to 4.5 K (Ghafarian et al., 2022).

Estimates on future soybean cropping opportunities in Europe have so far concentrated on the projection of soybean phenology under future climate conditions in Europe, using simple eco-physiological models or photothermal algorithms (Lamichhane et al., 2020; Schoving et al., 2020). Data-driven approaches suggest that the production potential in Europe will significantly increase in the future (Guilpart et al., 2022). However, two questions remain: First, to what extent will the southern border of the current suitability range also move to the north, when the risk of heat and drought makes some existing soybean production areas unprofitable? Second, what increase in soybean-growing potential can be expected as a result of expanded area, increased productivity via temperature and CO_2 changes, and the opportunity to grow higher-yielding varieties? To answer these questions, mechanistic agroecosystem models (AEMs) are required, which are constructed to predict plant growth and yield formation based on biophysical processes. In contrast to data-driven approaches, these models allow a profound analysis of yield-reducing factors that contribute to spatio-temporal patterns emerging from the simulations, and the consideration of different soybean maturity groups, given that their yield potential differs substantially.

The overall aim of this study was to assess Europe's future soybean production potential. The objectives were to (i) project the future distribution of recommended soybean maturity groups for maximum yield and yield stability in response to their demand for specific soil-climate conditions, (ii) simulate the productivity and potential area expansion under future climate conditions and (iii) analyse the most important yield-limiting climatic factors, that is, drought, heat, cold temperatures, length of the growing season and wet conditions during harvest, to identify areas with low production risk. All objectives were investigated using an ensemble of four robust mechanistic simulation models for soybean growth in a gridded simulation across Europe.

2 | MATERIALS AND METHODS

2.1 | Historical and future climate data

Observed and future projections of climate data were based on the data set developed by Webber et al. (2018). Daily gridded data (25 km^2) for the hindcast period (1980–2010) was obtained from

the Joint Research Centre's (JRC) Agri4Cast database (version 2.0) for the variables daily minimum, average and maximum surface air temperature, precipitation, 10-m wind speed, global radiation, and actual vapour pressure at 25 km spatial resolution for Europe covering the EU-27 countries plus UK, Croatia, Serbia, Bosnia and Herzegovina, Montenegro, Albania, North Macedonia, Norway, Liechtenstein and Switzerland. Wind speed was converted to an estimate at 2 m height following Allen and Wright (1997). Climate projections for the period 2040–2069 were constructed for five global climate models (GCMs: GFDL-CM3, GISS-E2-R, HadGEM2-ES, MIROC5 and MPI-ESM-MR) under the RCP4.5 and 8.5 forcing scenario. The climate projections were calculated using an enhanced delta change method that applies changes simulated by GCMs for aspects of temperature and precipitation variability in addition to changes in mean climate, as described in Ruane et al. (2015). Global radiation was increased by 10% when a wet day in the hindcast became dry in the scenario, and decreased by 10% when a dry day turned into a wet day. The five GCMs were selected out of a larger ensemble from CMIP5 (Taylor et al., 2012) to capture the likely range of regional climate changes projected in Europe following the approach described in Ruane and Mcdermid (2017). The climate data is available at https://doi.org/10.4228/zalf.vjcp-vep3. CO_2 concentrations in the crop models were fixed at 360 ppm for the hindcast, 499 ppm for the RCP 4.5 and 571 ppm for the RCP 8.5 scenario, respectively (Webber et al., 2018).

2.2 | Soil data

Soil data were obtained from the European Soil Database at 1 km^2 resolution (Hiederer, 2013). The data include organic carbon, bulk density, texture fractions and rooting depth for topsoil (0–30 cm) and subsoil layer (30 cm—lower boundary). The soil data can be accessed from the website of the Joint Research Centre at https://esdac.jrc.ec.europa.eu/content/european-soil-database-derived-data.

2.3 | Soybean data

Experimental data for model calibration and evaluation included 14 sites in France, Germany, Poland and Serbia, 13 years of observations (2006–2018), 21 cultivars from six maturity groups (II, I, 0, 00, 000, 0000), observations on crop management (irrigation, fertilisation, the dates of sowing) and phenological stages (crop emergence, the first flowers, the first pods, the first seeds, maturity and harvest), and productivity. All sites were controlled for weeds, pests and diseases. The grain yield ranged from 674 to 5402 kg ha^{-1}. The large majority of sowing dates ranged between 15 March and 15 May, with some exceptions for experimental reasons (to test early and late sowing dates); the harvest dates ranged from 17 August to 17 October. The data is available in the supplementary information (Table S1). Soil and weather data for the individual sites are provided in an open repository (https://github.com/zalf-rpm/soybeanEu-pub).

2.4 | Agroecosystem models

Agroecosystem models simulate crop growth and yield formation in response to weather, site conditions and management. The term 'yield' in the context of this study always refers to dry-matter soybean seed yield. Any attempt to relate the simulated yields reported here to actual farmers' yields needs to consider the remaining seed moisture at harvest, as well as the fact that soybean yields are affected not only by the interplay of weather and soil but also by micro-nutrient availability, weeds, pests, diseases and the management of these factors, which most AEMs do not consider. Beyond the capabilities of crop models, AEMs stand out by simulating continuous nutrient and water dynamics in the plant–soil system and the corresponding performance of different crops in sequence and long-term rotations, mimicking real agricultural production systems. Four well-established AEMs were selected for this study for their general ability to simulate soybean and to run massively parallel on a multi-core computer cluster.

All models include rigorously tested routines that enable them to reproduce the response of photosynthesis to temperature and atmospheric CO_2 concentrations, and of respiration and ontogenesis to temperature; water supply to the plant is simulated via well-tested approaches to simulate water movement in differently textured soils, soil water uptake via a depth-distributed rooting system and weather-related drivers controlling transpiration, including CO_2. Deficient water supply is considered to reduce plant growth via the photosynthesis and respiration pathway. All models also include a routine for representing biological nitrogen fixation in the soybean roots and additional uptake of mineral nitrogen from the soil. However, the models do not always include algorithms that reproduce the effects of critical heat or cold on specific physiological responses, such as flower abscission, seed cracking, pollen viability or stigma receptivity. This limitation will be addressed later. For more details on model development and testing for individual physiological processes, the reader is referred to the model documentation referred to in Table 1.

All models assume that the seed protein concentration will remain largely unaffected by elevated temperature and CO_2 levels, meaning that soybean yields translate directly into protein yields. Experimental evidence, however, indicates that soybean seed protein may decrease slightly under elevated CO_2 levels (Li et al., 2018; Soares et al., 2021).

2.5 | Model calibration

The AEMs have been calibrated and tested for simulating soybeans in Europe. APSIM (Holzworth et al., 2014) has been parameterised before for soybean in Australia (Denner et al., 1998; Robertson & Carberry, 1998) and the United States, covering MGs from 00 to VI (Archontoulis et al., 2014). MONICA (Nendel et al., 2011) has been previously parameterised to simulate soybean in Brazil, covering MGs ranging from VII to IX (Battisti, Parker, et al., 2017; Carauta et al., 2018; Hampf et al., 2020). HERMES (Kersebaum, 2007) exhibits

TABLE 1 Agroecosystem model versions and availability

Model	Version	Source
APSIM (Holzworth et al., 2014)	7.9	https://www.apsim.info/download-apsim/downloads/
MONICA (Nendel et al., 2011)	3.2.6.195	https://github.com/zalf-rpm/monica/releases/tag/3.2.6.195
HERMES (Kersebaum, 2007)	Hermes2Go v0.1.0	https://github.com/zalf-rpm/Hermes2Go/releases/tag/v0.1.0
STICS (Brisson et al., 2003)	Stics-9.0	https://www6.paca.inrae.fr/stics_eng/Download

a crop module similar to MONICA and has been parameterised once for maize–soybean crop rotation in Iowa, USA (Malone et al., 2017) for soybean varieties of MG II. However, it was first calibrated for different soybean MGs using the data provided for this calibration exercise. STICS (Brisson et al., 2003) has been calibrated and tested for soybean MGs 00 to II in Canada (Jégo et al., 2010) and a range of MGs in southern France (Schoving et al., 2022). APSIM, MONICA and STICS also underwent joint testing against further data sets within an AgMIP model intercomparison exercise (Kothari et al., 2022).

The following indices were used to evaluate model performance:

The *root-mean-square error* (RMSE) describes in absolute terms the deviation between predicted and observed values. It was calculated as:

$$\mathrm{RMSE} = \sqrt{\frac{1}{n}\sum_{i=1}^{n}(P_i - O_i)^2}, \tag{1}$$

where n is the number of treatments, P_i represents the estimate of the ith treatment, and O_i represents the ith observed value. This error metric is preferred for normally distributed data (Hodson, 2022).

The *mean bias error* (MBE) was used as an indicator of the direction and magnitude of bias, signifying a systematic under- or over-prediction of the model. It was calculated as:

$$\mathrm{MBE} = \frac{1}{n}\sum_{i=1}^{n}(P_i - O_i). \tag{2}$$

The refined version of Willmott's Index of Agreement (d_r) (Willmott et al., 2012) uses error variances, not absolute errors, and is seen as a goodness-of-fit indicator. It was calculated as:

$$d_r = \begin{cases} 1 - \dfrac{\sum_{i=1}^{n}|P_i - O_i|}{2\sum_{i=1}^{n}\left|O_i - \overline{O}\right|}, \text{when} \\ \sum_{i=1}^{n}|P_i - O_i| \le 2\sum_{i=1}^{n}\left|O_i - \overline{O}\right| \\ \dfrac{2\sum_{i=1}^{n}\left|O_i - \overline{O}\right|}{\sum_{i=1}^{n}|P_i - O_i|} - 1, \text{when} \\ \sum_{i=1}^{n}|P_i - O_i| > 2\sum_{i=1}^{n}\left|O_i - \overline{O}\right| \end{cases} \tag{3}$$

where $\bar{O}$ represents the average observed value for all treatments. Ranging in [0; 1], this indicator yields 1.0 in the case of perfect agreement.

For this particular study, all four AEMs were provided with yield and phenology data from the experimental data across multiple sites and years (Table S1). The data set was split by MG to receive two independent data sets with a similar number of site × year combinations for calibration and testing (Table 2). These MGs cover the soybean varieties currently grown across Europe. No yield and phenology data is currently available from Europe for MG III, which is likely to be introduced to this continent within the period covered by this study. Modellers extrapolated MG III parameters based on their experience with soybean grown in the United States. Further details on the calibration and testing data set and on the calibration procedure for the individual models are provided in the supplementary material. Calibration and testing results for the individual models are displayed in Figure 1; the respective performance indicators are displayed in Table 2. The performance indicators show an RSME ranging from 467 to 1274 kg ha^{-1} (90% quantiles) for soybean dry matter seed yield across all models and MGs using the independent test data set, which is considered a good result for the range of soybean varieties considered (compare Kothari et al., 2022). Applying four suitable models in ensemble mode further reduces the prediction error considerably (Martre et al., 2015; Wallach et al., 2018).

2.6 | Agroecosystem model simulations

For each of the grid cells, we applied the models using all six soybean variety parameterisations (0000–II) and including a seventh (III) for future scenarios. The AEMs triggered soybean sowing each season between 15 March and 15 May when air temperature exceeded 9°C (7 days moving average) and soil temperature exceeded 7°C (5 days moving average). This is a one degree lower threshold, as known for later MGs (III–V; Alsajri et al., 2019), owing to the cold-temperature adaptation of the earlier MGs (Ritter & Bykova, 2021). Harvest was triggered at simulated maturity. The models were run in continuous mode for 30 years for a 1 km^2 grid across Europe for each maturity group, without any fertiliser application for soybean, in rotation with medium-maturing maize (standard variety in each of the models) to mimic appropriate soil moisture conditions at the beginning of the season across the different climate zones of Europe. Two simulations were run; one starting with soybean in the first year followed by maize in the second year, and another covering the opposite combination, so that for each of the 30 years soybean yield was available for analysis. Each 30-year simulation was preceded by a one-season spin-up period to ensure soil moisture levels that are representative

TABLE 2 Performance indices for the agroecosystem models APSIM, MONICA, HERMES and STICS for simulating soybean varieties of maturity group 0000–II for different locations and seasons across Europe. Phenology indices evaluate observed and simulated DOY for seed emergence, the beginning of flowering (R1), the appearance of the first pod (R3) and beginning of pod maturity (R7) for each maturity group (STICS does not explicitly simulate R3). Yield performance indices evaluate observed and simulated dry matter seed yields, respectively

	Calibration						Testing					
Maturity group	**MG 0000**	**MG 000**	**MG 00**	**MG 0**	**MG I**	**MG II**	**MG 0000**	**MG 000**	**MG 00**	**MG 0**	**MG I**	**MG II**
Varieties	Augusta	Sultana	Merkur	Princeza, Galina	Isidor	Ecudor	Erica, Paradis	Merlin, Lissabon	Taijfun, Fortuna	Valjevka, Proteinka	Balkan, Sava	Rubin, Vojvođanka
Countries	Poland	France, Germany	Serbia	Serbia	France	France	Poland	Germany, Poland	Serbia	Serbia	Serbia	Serbia
No. phenology	24	45	0	22	51	50	36	38	0	10	71	63
No. yield	6	11	5	20	13	13	9	13	4	22	27	22
Mean observed yield ($kg\,ha^{-1}$)	3135	3139	3172	2675	3538	4302	3070	3605	2434	3629	3080	3021
APSIM												
Phenology												
RMSE (day)	12.9	10.1	–	10.1	12.1	17.9	16.5	11.5	–	9.7	13.8	12.9
MBE (day)	10.7	5.2	–	−6.1	0.1	7.7	14.3	7.9	–	−4.7	−4.8	2.2
d_r	0.79	0.98	–	0.91	0.88	0.87	0.74	0.84	–	0.93	0.91	0.94
Yield												
RMSE ($kg\,ha^{-1}$)	754.8	704.1	1176.3	678.4	590.0	871.7	946.8	711.5	354.7	1129.0	781.5	688.3
MBE ($kg\,ha^{-1}$)	555.1	−350.4	−206.6	−90.8	−34.4	−684.8	578.0	−198.7	110.2	−767.4	−136.0	−330.6
d_r	0.91	0.92	0.86	0.91	0.93	0.91	0.49	0.67	0.86	0.38	0.66	0.71
MONICA												
Phenology												
RMSE (day)	8.1	9.7	–	2.3	7.7	9.2	8.0	5.4	–	2.6	9.4	9.1
MBE (day)	0.2	−0.7	–	0.7	2.9	2.8	−0.9	−0.2	–	1.2	−1.9	−3.1
d_r	0.87	0.88	–	0.98	0.92	0.90	0.87	0.94	–	0.98	0.93	0.92
Yield												
RMSE ($kg\,ha^{-1}$)	567.0	696.6	1181.3	725.8	1343.7	634.7	773.1	815.8	417.1	1270.2	953.0	816.1
MBE ($kg\,ha^{-1}$)	46.8	89.1	−288.1	−42.5	619.5	73.3	173.6	24.1	−271.9	−646.2	−509.6	8.8
d_r	0.81	0.75	0.66	0.83	0.52	0.59	0.51	0.75	0.60	0.62	0.58	0.64

TABLE 2 (Continued)

	Calibration						Testing					
Maturity group	MG 0000	MG 000	MG 00	MG 0	MG I	MG II	MG 0000	MG 000	MG 00	MG 0	MG I	MG II
HERMES												
Phenology												
RMSE (day)	6.8	10.6	—	9.7	6.9	10.9	8.4	11.7	—	9.1	14.7	13.4
MBE (day)	2.8	2.7	—	−6.4	0.7	3.0	1.8	5.9	—	−5.9	−5.8	−2.2
d_r	0.89	0.98	—	0.93	0.93	0.92	0.89	0.86	—	0.94	0.90	0.91
Yield												
RMSE (kg ha^{-1})	1066.5	977.6	1438.1	1025.3	1176.4	968.0	913.9	1052.4	337.2	1394.9	879.0	771.3
MBE (kg ha^{-1})	−115.5	−844.3	−449.0	29.1	161.0	−11.8	−218.5	−827.4	95.8	−731.1	−510.5	−357.5
d_r	0.57	0.64	0.60	0.76	0.45	0.56	0.53	0.48	0.86	0.24	0.65	0.68
STICS												
Phenology												
RMSE (day)	7.9	6.9	—	17.2	12.2	17.9	9.6	8.8	—	17.4	13.2	14.2
MBE (day)	−1.1	1.4	—	−7.7	0.1	7.7	−2.6	−0.8	—	−7.9	0.3	0.4
d_r	0.89	0.93	—	0.86	0.88	0.87	0.86	0.89	—	0.91	0.90	0.97
Yield												
RMSE (kg ha^{-1})	887.1	618.8	1296.1	1068.7	1166.0	1849.2	1023.6	804.2	582.3	1076.9	1275.6	1277.2
MBE (kg ha^{-1})	645.0	319.2	143.0	−91.6	−339.6	−439.3	710.0	−16.5	−0.5	22.6	−469.9	−555.9
d_r	0.89	0.93	0.84	0.84	0.86	0.83	0.52	0.80	0.51	0.71	0.52	0.48

Abbreviations: d_r, the refined version of Willmott's Index of Agreement; MBE, mean bias error; RMSE, root mean square error.

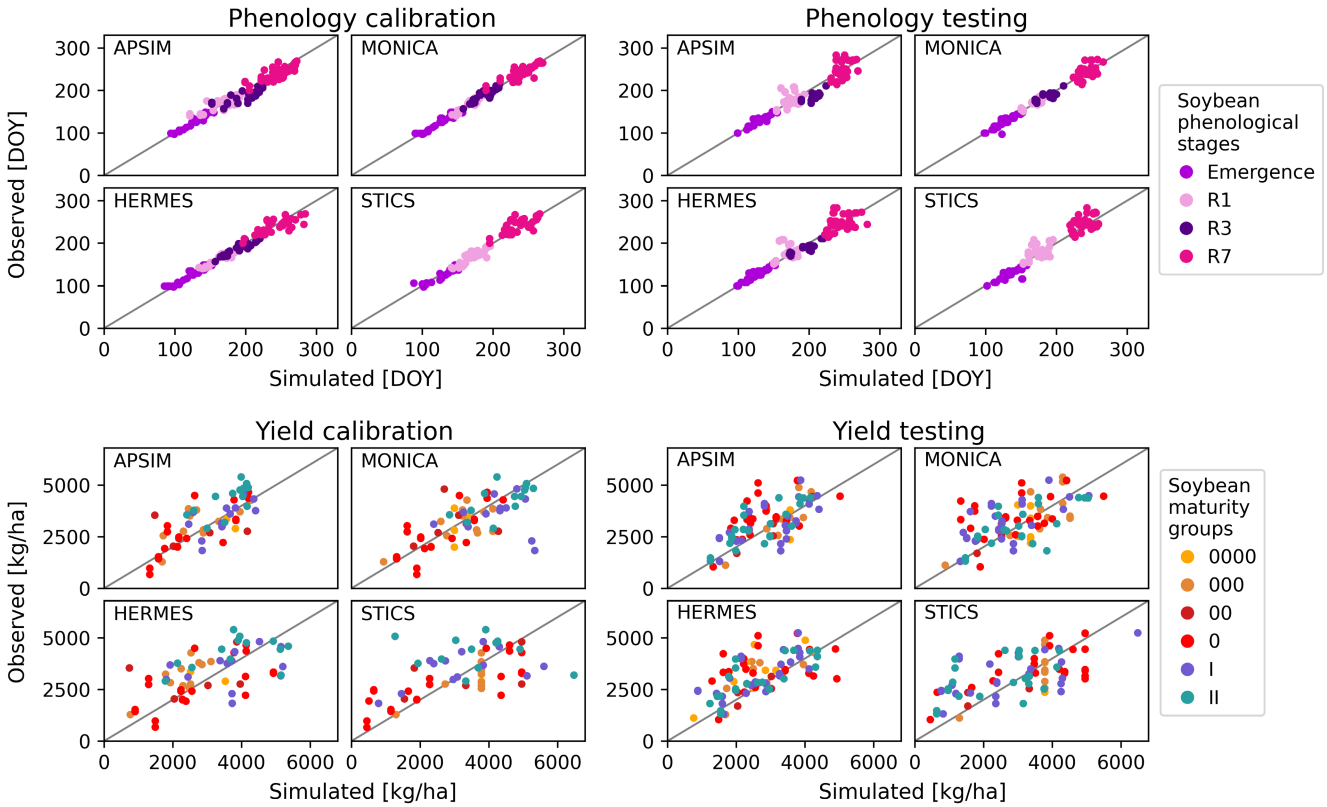

FIGURE 1 Calibration and testing of the four agroecosystem models APSIM, MONICA, HERMES and STICS against soybean data from various sites across Europe. Phenology results include dates for seed emergence, the beginning of flowering (R1), the appearance of the first pod (R3) and beginning of pod maturity (R7), and integrate over all maturity groups (STICS does not explicitly simulate R3). Yield results show dry matter seed yields for each maturity group separately. The solid line signifies equality between simulated and observed values.

of the respective pixel. The maize crop is supplied with sufficient fertiliser to grow, either by automatically calculated fertiliser applications or by inactivating the nitrogen response function, allowing for a plausible simulation of the water uptake by an optimally managed maize and the accumulation of soil moisture deficit between crops in the rotation when consecutive drought years occur. The first set of simulations was conducted for rainfed conditions, the second with additional rule-based irrigation (water being added whenever the simulated soil moisture falls below a defined model-specific threshold value) being activated to ensure optimal water supply for producing potential yields. Since not all models are equipped with suitable algorithms for simulating blossom drop or seed cracking, these responses were, therefore, analysed separately based on only weather data for the identification of production risk from low temperatures around flowering. This also applies to the model's ability to simulate heat stress. Since not all models are equipped with suitable heat stress algorithms, heat stress was identified from high temperatures during flowering and pod setting. Furthermore, not all models are equipped with algorithms that delay the harvest trigger on the basis of soil moisture being at or above field capacity to represent field trafficability. We again remain with only a meteorological rule, also to integrate other reasons why farmers would not harvest a wet crop: combine harvesters would clog, impeding a quick harvest, and wet seeds would require post-harvest drying, which is expensive. The rainfall-related rule is a compromise to represent all these issues with rain falling at harvest time.

2.7 | Data analysis—Yields and maturity groups

For each individual AEM, we identified the MG that produced the highest yields in each grid cell pixel. According to previous agronomic knowledge, MGs that (i) did not mature before 15 October, (ii) produced less than 900 kg ha^{-1} or (iii) produced less than 20% of the average yield across MGs in 3 out of 30 years were considered as yield failure and assigned 'na' in the particular grid cell. These quality criteria represent the assumption that farmers would not grow a maturity group that does not mature in time or is at >10% risk of a severe yield failure. The MG with the highest yield and lowest standard deviation was selected from the remaining MGs. This MG reflects the farmer's desire for higher yield stability. If none of the six MGs passed the quality criteria, the yield was reported as 'na'. The median MG across the five GCMs was then selected. If two MGs were equally frequent, the one with the highest number of the same MG in the surrounding grid cells was selected (moving window). To display the yield per grid cell, the yield of the respective best-performing MG was averaged over the GCMs and the standard error indicating the uncertainty emanating from the GCM selection was calculated.

In a subsequent step, the yield per grid cell was averaged over the AEMs. In the end, each grid cell displays a yield value that emerged from a 5 GCM×4 AEM ensemble for the future scenario, and a 4 AEM ensemble for the hindcast. We further combined rainfed and irrigated soybean simulations into one map, using the MIRCA2000 (Portmann et al., 2010) data set for irrigated soybean as a mask (Figure 2) in such a way that grid cells in irrigated areas presume production under 100% irrigation. The mask was equally applied for the historic and future applications since no qualified assumption for future distribution of irrigation practices is at hand. This approach reflects the fact that, in high-yielding soybean production areas in Europe, supplementary irrigation is frequently applied. Pixels identified as being at risk of cold snaps or too wet conditions at harvest (see below) were reported with zero yield.

For the summary, yields were weighed by the share of agricultural land in each pixel as provided by the Earthstat (2000) data set (Ramankutty et al., 2008), and then summed up across pixels. For the future scenario, we remain with the same assumption for the distribution of agricultural land across Europe.

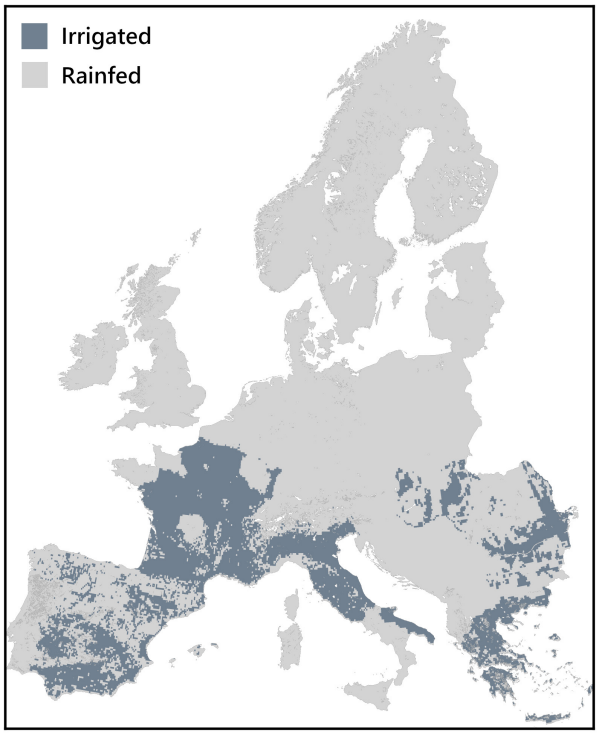

FIGURE 2 MIRCA2000 mask for the irrigated soybean area (Portmann et al., 2010).

2.8 | Data analysis—Production risk

We identified five major risk factors for soybean production in Europe from previous agronomic knowledge: drought, heat, season length, cold snaps around flowering, and rainfall during the harvest period. Drought and season length were derived from the AEM simulations, while heat stress, cold snaps and wet harvest conditions were extracted directly from the climate data. We display a pixel as being potentially under risk of drought if the rainfed yield falls below 2.0 $t\,ha^{-1}$ and irrigated yield simultaneously exceeded the rainfed yield by 50%. An overly short season as a limiting factor is flagged if the soybean does not reach maturity before 15 October in six or more seasons out of 30. For this study, we assumed that heat stress causes significant damage when the photoperiod air temperature within 32 days after the first simulated day of flowering exceeds 30°C for at least 3 days, and becomes relevant for farmers' decision-making when this happens in 6 or more out of 30 years. The photoperiod air temperature (T_{photo}) calculates as

$$T_{photo} = T_{max} - \frac{T_{max} - T_{min}}{4}, \quad (4)$$

where T_{max} is the maximum and T_{min} is the minimum daily air temperature measured at 2 m height above the ground (Mirschel & Wenkel, 2007).

Cold snaps are defined as the minimum temperature in July and August falling below +5°C once in 6 or more out of 30 years. Finally, too wet harvest conditions are exhibited if rain falls within 10 days of soybean maturity in 10 years or more out of 30 years. A dry period of two or more consecutive days overrules this criterion. There is little quantifiable evidence in the literature for many of the crop failure conditions used here for this study, and yet these effects exist. We see our approach as a first attempt to visualise these effects and hope to be challenged by other research groups that come up later with better-suited algorithms.

2.9 | Data analysis—Uncertainty

As a measure of uncertainty, the standard deviation of the yields simulated using the AEMs was apportioned into a contribution of the AEMs and the underlying GCMs. Uncertainty caused by the AEMs was calculated as the standard deviation of the AEMs separate for each individual GCM, and then averaged across the GCMs. The uncertainty caused by the GCMs was calculated from individual AEMs simulating all GCMs and then averaged across the AEMs.

2.10 | Data analysis—Deconstructing physiological and adaptation effects

In a bid to identify the share of the MG adaptation in the overall productivity gain, we compared the simulated future scenarios against a simulation in which the MGs remained constant in each pixel, that is, for those pixels identified as soybean growing area in the hindcast, we applied future climate scenarios without changing the MG. A positive difference between the respective climate scenario and the hindcast was then interpreted as the yield gain that emerges from plant physiological processes directly responding to the elevated temperature and CO_2 levels. Subtracting this from the difference between hindcast and

future climate scenarios for the simulations in which farmers chose an MG with higher heat requirement and yield potential gives the yield gain caused by the adaptation only. Division by the total yield gain (physiological plus adaptation effect) results in the share of the adaptation effect in the total yield gain (Equation 5). Negative yield differences also occurred, despite the choice of a longer-growing MG. In this case, the decision to use a better-suited MG prevented an even higher yield loss. In some cases, the algorithm also chose a different MG for a more stable yield over time. These cases were not further analysed.

$$AE = \frac{(Y_f - Y_b) - (Y_{bf} - Y_b)}{Y_f - Y_b} \times 100\,\%, \quad (5)$$

where AE is the share of the adaptation effect in the total yield gain, Y_b is the soybean yield in the hindcast, Y_f is the yield in the future climate scenarios with adaptation, and Y_{bf} is the yield in the future climate scenarios with constant MG.

3 | RESULTS

3.1 | Projected maturity group distributions, yields and production risks

We found that the simulated current distribution of soybean maturity groups across the European continent was plausible, with MG 0000 being grown in the coastal areas bordering the Baltic Sea and the North Sea to the south (Figure 3a), albeit with unprofitable yield expectations (<0.9 $t\,ha^{-1}$, Figure 4a), with the later MGs appearing gradually towards the south, and with MG II appearing in distinct areas scattered around the Mediterranean and the Balkan area (Figure 3a). The highest average yields of >4.5 $t\,ha^{-1}$ were simulated in irrigated areas in central and western France, northern Italy and Romania, which closely reflect current soybean production areas (Figure 4a). Production limits were imposed by drought in large areas south of 42°N latitude (south of 48°N latitude in eastern Europe, apart from the Dinaric Alps), and an overly short season in southern England, the coastal areas around the Baltic Sea, and higher-elevation areas in Central Europe (where cold snaps would also pose a risk; Figure 5a). Rain at harvest was mainly a risk on the British Isles and in Brittany, and cold temperatures also limited production in Scandinavia (Figure 5a). Heat was identified as a risk only in smaller areas in the Po Valley and the great Hungarian plain.

Under climate scenarios for the period 2040–2069 for radiative forcing of 4.5 Wm^{-2} (RCP 4.5, Figure 3b), the simulated MG distribution shifted northwards, allowing for MGs 000 and 00 in coastal areas of southern Sweden and Finland, while MG 0000 decreased in importance. MG III appeared in the southern parts of the Mediterranean countries. The projections revealed economically viable yields (2–3 $t\,ha^{-1}$) in England, Denmark and the Baltic states (Figure 4b), where the risk to production was also projected to become negligible (Figure 5b). In Central Europe, production risks due to cold temperatures remained only in highland areas and mountain ranges. In France and eastern Europe, the projected drought risk increased, while the risk of heat stress emerged mainly in France, the Po Valley and the Pannonian Basin (Figure 5b).

For the same future period, but based on radiative forcing of 8.5 Wm^{-2} (RCP 8.5, Figure 3c), the MG 0000 has almost vanished, while MG 0 comes out as the better choice more prominently in Poland, Sweden and Finland. South of the Po Valley in Italy, MG 00 outperforms MG 0, which was the better-performing MG under the RCP 4.5 scenario, demonstrating a reverse development under increasing temperature, despite being irrigated. In addition, MG III is no longer the preferred selection in Apulia under RCP 8.5, in contrast to the RCP 4.5 scenario, and does not gain further importance in other regions either (Figure 3c). The yield levels and the production risk remained virtually unchanged from RCP 4.5 to RCP 8.5 (Figures 4c and 5c). Only the risk due to heat stress is projected to further increase under RCP 8.5.

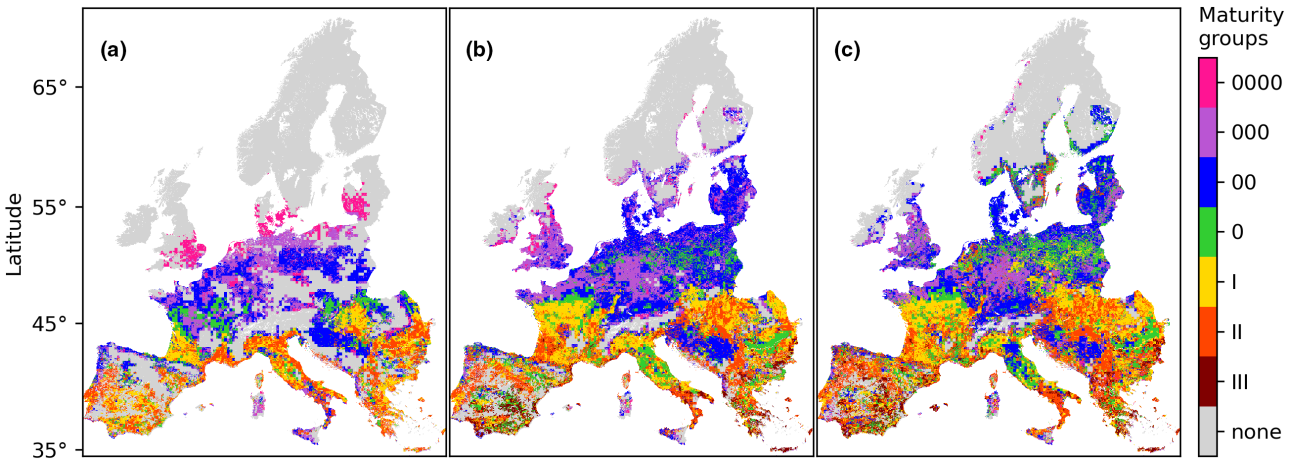

FIGURE 3 The soybean maturity group (0000—Extremely early; III—Middle) that produced the highest yield in individual pixels in a simulation of an ensemble of four crop models. 1981–2010 hindcast (a), 2040–2069 RCP 4.5 scenario ensemble mean of five global climate models (b), 2040–2069 RCP 8.5 scenario ensemble mean of five global climate models (c). Note that MG III was only introduced for the future scenarios.

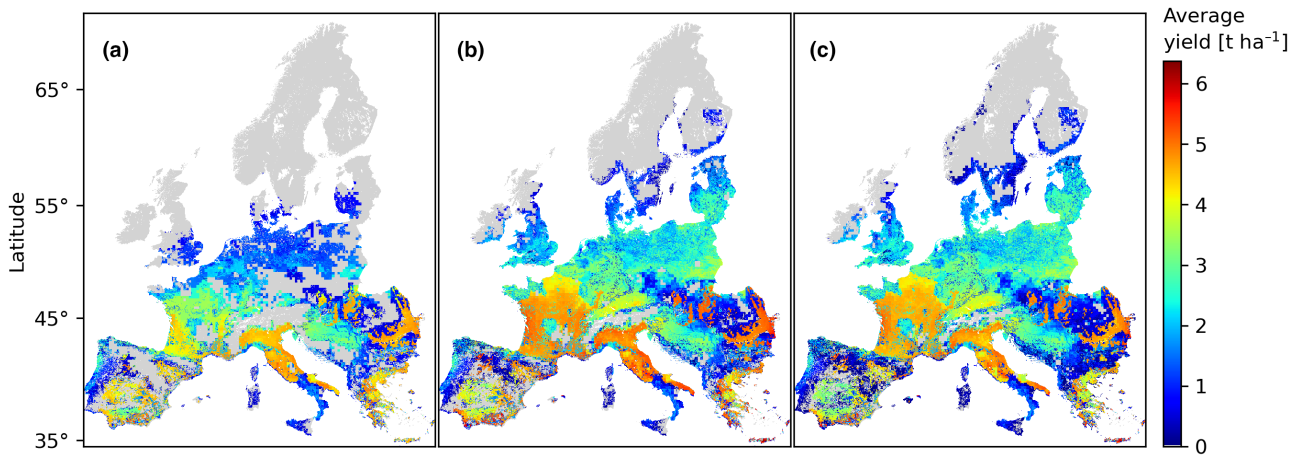

FIGURE 4 Soybean dry matter seed yields in Europe as simulated by an ensemble of four crop models. 1981–2010 hindcast (a), 2040–2069 RCP 4.5 scenario ensemble mean of five global climate models (b), 2040–2069 RCP 8.5 scenario ensemble mean of five global climate models (c).

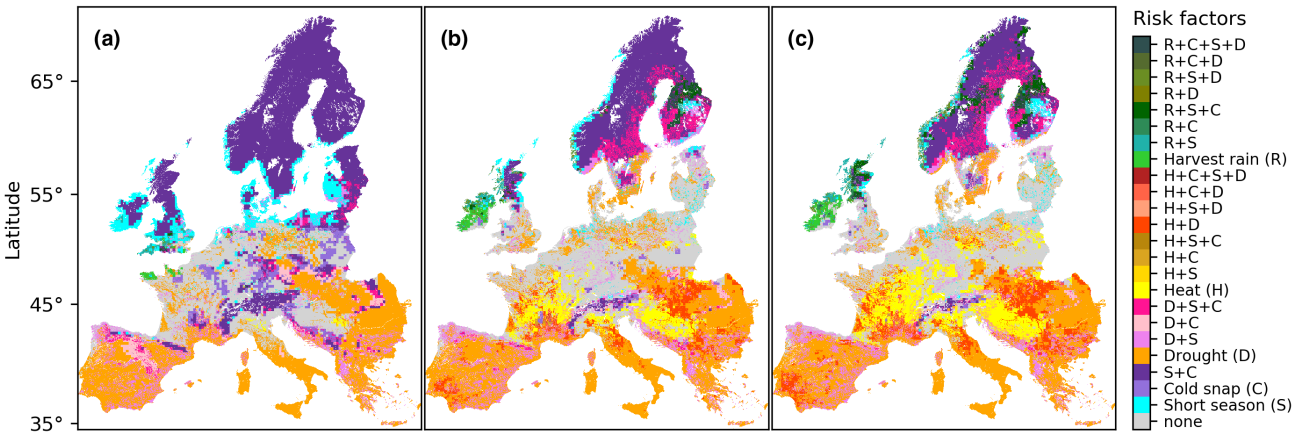

FIGURE 5 Soybean yield failure risk due to drought (D), heat above 30°C during flowering (H), overly short season (S), overly wet conditions during harvest (R) and cold snaps below 5°C during July and august (c), and their compound effects. 1981–2010 hindcast (a), 2040–2069 RCP 4.5 scenario ensemble mean of five global climate models (b), 2040–2069 RCP 8.5 scenario ensemble mean of five global climate models (c).

The simulations suggest that the suitability for certain soybean maturity groups will move northward along the latitudinal gradient of Europe (Figure 6). While soybean yields were simulated to increase under future climate scenarios above 45°N latitude compared with historic climate conditions, they tend to decrease further south (Figure 7). The risk of cold snaps is projected to decrease constantly under future climate scenarios across Europe. At the same time, drought risk is expected to increase significantly in northern areas above 50° latitude, while southern areas are already at high risk of drought (Figure 8). The risk of rain during harvesting increased significantly in the simulations under future climate scenarios in central and northern areas, and the risk of an overly short season decreased for areas between 45° and 60° latitude (Figure 8). The risk of heat stress impairing production is projected to increase drastically between 40° and 53° latitude in both future scenarios, but to a more pronounced extent in the RCP 8.5 projection (Figure 8).

Across Europe, productivity under rainfed conditions increased from 1.4 to 1.7–1.9 t ha^{-1} from historic to future climate scenarios, and under irrigation from 3.9 to 4.2 t ha^{-1}, respectively (Table 3). The suitable production area increased by 54%–65% and 5%–6% for rainfed and irrigated systems, respectively. However, the area under drought risk increased by 28%–29% in large parts of Europe; rain during harvest increased in certain areas such as Ireland. Short seasons and cold snaps during flowering decreased by 29%–33% and 46%–54%, respectively. Heat stress, which plays no significant role in the historic simulations, emerges on 590,000–925,000 km^2 in the future climate scenarios (Table 3).

3.2 | Uncertainty of simulations

The standard deviation across Europe of the AEM ensemble is 1080 kg ha^{-1} for the historical time slice, and for the full GCM × AEM

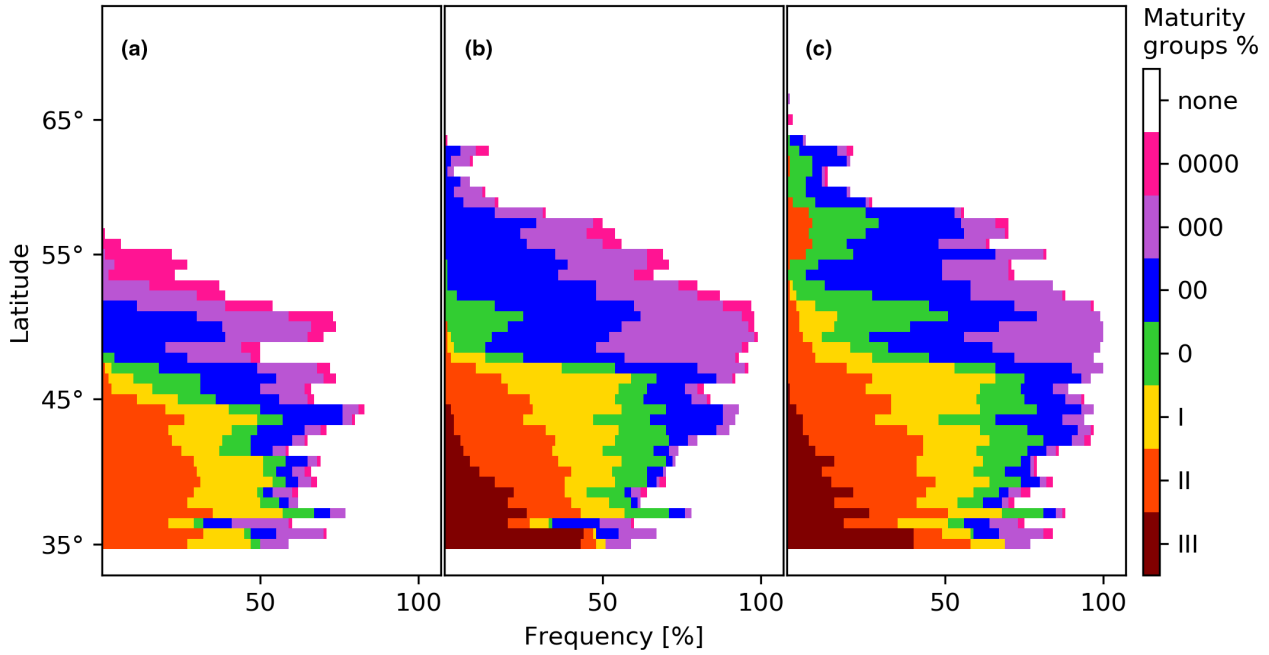

FIGURE 6 Frequency distribution for soybean maturity groups along the latitudinal gradient of Europe created from the hindcast (a), the RCP 4.5 (b) and the RCP8.5 (c) scenario simulations.

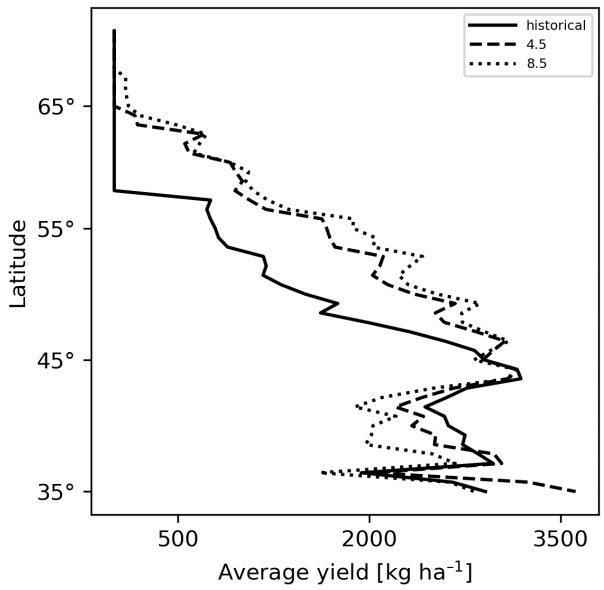

FIGURE 7 Frequency distribution for soybean yields along the latitudinal gradient of Europe created from the hindcast (━), the RCP 4.5 (┅) and the RCP8.5 (…) scenario simulations.

ensemble 1060 kg ha^{-1} and 1090 kg ha^{-1} under the RCP 4.5 (Figure 9a) and RCP 8.5 future scenario, respectively. Across the GCMs only, the standard deviation amounts to 460 kg ha^{-1} (RCP 4.5, Figure 9b) and 500 kg ha^{-1} (RCP 8.5) for the future period, with slightly higher deviations in southern Poland and Moravia; across the AEMs, the standard deviation amounts to 1040 kg ha^{-1} (RCP 4.5, Figure 9c) and 1060 kg ha^{-1} (RCP 8.5) for the future period, with higher deviations in Estonia, Wales, southeast France and southeast Spain. The spatial pattern of uncertainty does not change significantly from RCP 4.5 to RCP 8.5. In areas where soybean was irrigated (Figure 2), uncertainty across the AEMs was significantly reduced (Figure 9c).

3.3 | Deconstructing physiological and adaptation effects

Comparing the simulated future scenarios against a simulation in which the MGs remained constant in each pixel showed that cultivation of a long-maturing variety was most effective in areas where today's climate would already allow for growing 0 or 00 varieties (Figure 3a). Here, the share of the adaptation effect in the total yield gain often exceeded 50% (Figure 10). In areas where the season length was previously a limiting factor for growing soybeans in the historical period (Figure 5a), or where the yield level already exceeded 4 t ha^{-1} (Figure 4a), higher yields are often predominantly explained by physiological effects, despite the use of cultivars in higher MGs (Figure 10). In historically very high-yielding areas (Figure 4a), no further yield gain was achieved.

4 | DISCUSSION

For the current climatic situation, the model ensemble simulated a suitable production area for soybean of 86 Mha (860,000 km^2), with an average yield of 2.52 t ha^{-1} and a minimum yield of 0.9 t ha^{-1}. Using a data-driven approach, Guilpart et al. (2022) flagged >200 Mha suitable for soybean production, with yields higher than 1.5 t ha^{-1}, albeit including Ukraine, Turkey, the Caucasus region and parts of Russia, which were not considered in our study. If an area of 86 Mha were

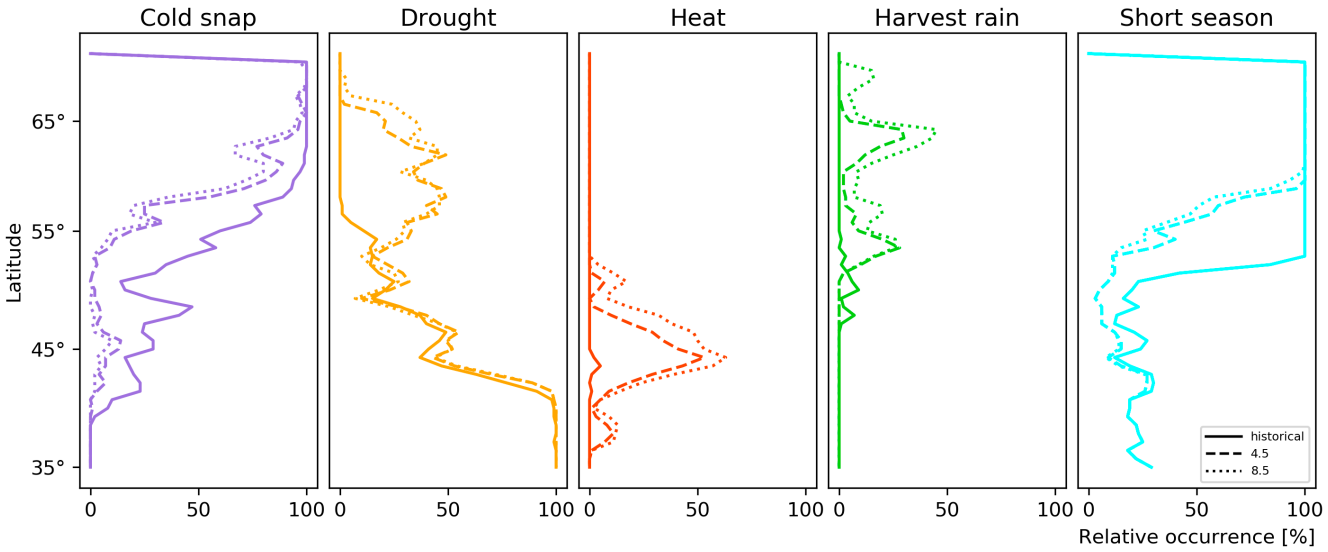

FIGURE 8 Frequency distribution for risk factors to soybean production along the latitudinal gradient of Europe created from the hindcast (━), the RCP 4.5 (▪▪▪) and the RCP8.5 (…) scenario simulations.

TABLE 3 Potential soybean productivity (dry matter seed yield per hectare) and production area. Note that the areas reported here were calculated using the share of agricultural land per pixel as reported by Ramankutty et al. (2008)

	1981–2010	2040–2069 RCP 4.5	Percentage change	2040–2069 RCP 8.5	Percentage change
Average productivity (t ha^{-1})					
Rainfed	1.40	1.86	32.9 ↗	1.69	20.7 ↗
Irrigated	3.86	4.21	9.1 →	4.24	10.0 →
Total	2.52	2.73	8.3 →	2.74	8.7 →
Suitable production area (1000 km^2)					
Rainfed	466	716	53.5 ↑	768	64.7 ↑
Irrigated	394	414	5.3 →	416	5.7 →
Total	860	1130	31.4 ↗	1184	37.7 ↗
Area under production risk (1000 km^2)					
Drought	1857	2393	28.9 ↗	2378	28.1 ↗
Heat	16	590	3687.5 ↑	925	5781.3 ↑
Short season	2316	1640	−29.2 ↘	1559	−32.7 ↘
Harvest rain	48	159	231.3 ↑	278	479.2 ↑
Cold snap	1990	1073	−46.1 ↘	912	−54.2 ↓

cropped with soybean in only one out of 5 years, 43 million tonnes of soybean could be produced, which represents 74% of the 58 million tonnes of soybean grain imported in 2009–2013 (FAOSTAT, 2019). One out of 5 years, however, is what we would consider the maximum of what could practically be implemented, with large variation across Europe. We assume that (i) southern European cropping systems could include a higher share of, for example one out of 2–4 years of soybean in rotations, while northern cropping systems would tolerate only one out of 4–5 years (Notz et al., under revision), and that (ii) the required market opportunities and processing capacities are available. The reason for the low share of soybean in northern cropping systems is that winter cereals are more competitive and produce the highest and most stable yields (Reckling et al., 2018). Soybean overlaps with winter crops, which must be sown in early autumn when soybean is still in the field. These winter crops are still important constituents in northern rotations not only for meeting market demands but also for controlling disease and nitrate leaching. In the south, the higher yield potential makes soybean an economically stronger candidate, which could be grown in alternation with grain maize. Under future climate scenarios, the ensemble estimated that the suitable area would increase significantly by 31%–38%, adding another 12–15 million tonnes of soybean according to the above-used scheme. In addition, productivity would rise slightly by 3%–5% (1.6–2.9 million tonnes), resulting in a further increase in potential production in the range of 56–61 million tonnes. This potential production is approximately the amount currently imported to the EU. Guilpart et al. (2022) suggested that a self-sufficiency level of 50%–100% could be achieved in Europe under historical and

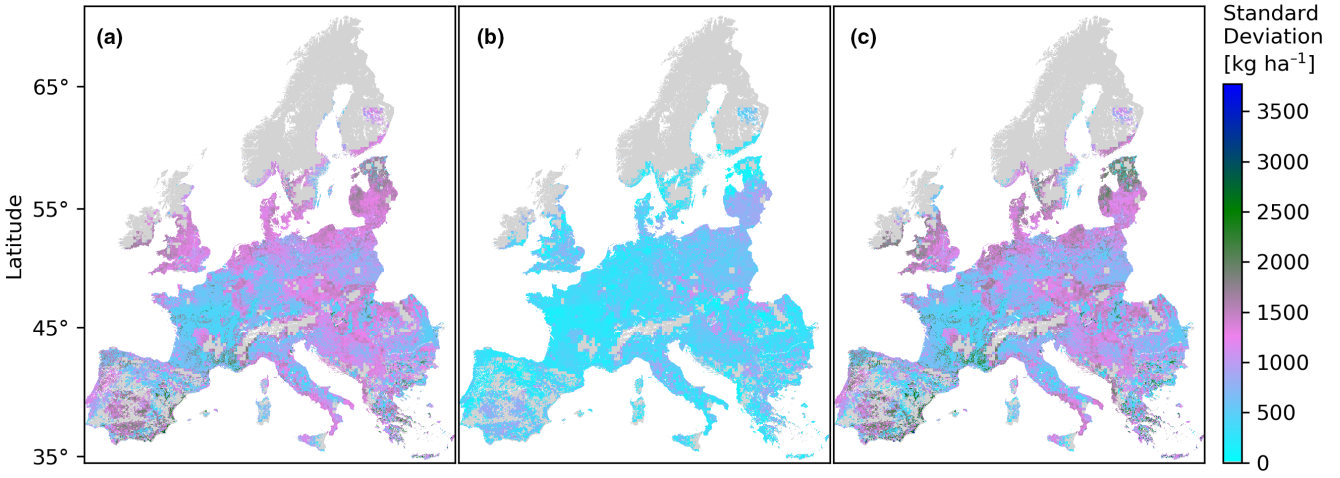

FIGURE 9 Standard deviation of soybean dry matter seed yields in (kg ha^{-1}) of the complete ensemble of climate and soybean models (a) as a measure of uncertainty of the ensemble prediction, and breakdown into the contribution of the global climate models (b) and the agroecosystem models (c) for RCP 4.5. Grey areas indicate no soybean production.

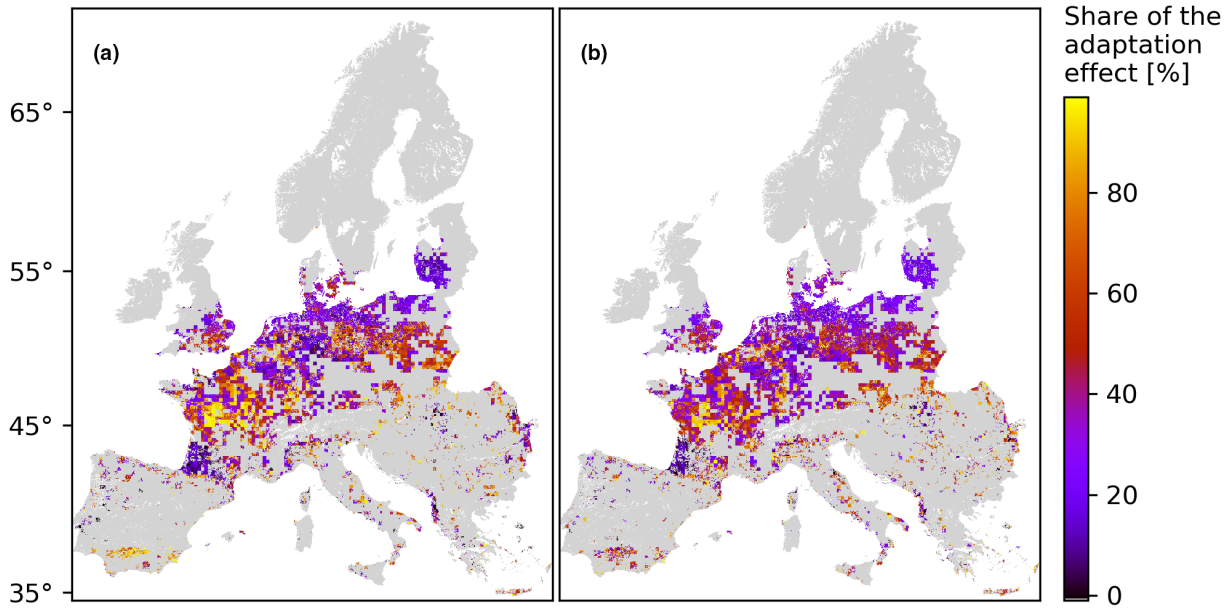

FIGURE 10 Share of the yield gain (future versus historic) resulting from the use of a better adapted maturity group in the total future yield gain, which also includes the physiological response of the soybean to elevated temperature and CO_2 levels (adaptation effect), for RCP 4.5 (a) and RCP 8.5 (b).

future climate scenarios if 4%–12% of the current European cropland was dedicated to soybean cultivation. Since we did not consider production in Ukraine, Turkey, the Caucasus region and Russia in our study, almost all of the remaining area suitable for soybean production would have to be used to meet the EU's self-sufficiency goals. Assuming that future heat stress will substantially reduce productivity in large parts of today's high-yielding areas (an effect that we have not yet quantified in our simulations), it may not be possible to meet EU demands using EU territory alone. In summary, we were able to show that the increase in productivity due to more area becoming suitable for growing soybean because of improved climatic conditions by 2040–2069 in the central and northern parts of Europe is higher than the yield-declining effect of the expected increasing drought risk (Gray et al., 2016) in the southern and eastern parts of Europe, if summarised for the whole of Europe. However, for southern parts of Europe, the regional consequences of climate change may result in severely reduced production potentials.

Individual studies have indicated the potential to cultivate soybean in areas where the crop is currently rarely grown. Towards the north, such studies found suitable varieties and management combinations for successful growth in southwest Poland (Serafin-Andrzejewska et al., 2021), northern Germany (Karges et al., 2022; Kühling et al., 2018), Belgium (Pannecoucque et al., 2022), the UK (Coleman et al., 2021) and southern Sweden (ongoing). The study

by Coleman et al. (2021) revealed that under current climate conditions, early-maturing varieties will mature in the south of the UK, while the probability of failure will increase with latitude, supporting our simulations (Figure 4a). Towards the south, studies show a high soybean productivity, for example in northern Spain (Simon-Miquel et al., 2021), where the crop has not yet been cultivated due to the prevailing specialisation in highly productive maize. Our assessment is the first one at the European scale that simulates soil–crop–climate processes using detailed agronomic constraints, identifying the major factors that drive risks in production (Figure 5).

Our simulations suggest a clear geographical shift of soybean maturity groups along the latitudinal gradient of Europe, from the historic simulation to both future scenarios (Figure 6). This shift would allow farmers to grow higher-yielding MGs in areas where extremely early and, therefore, low-yielding genotypes are used today. The areas with the highest yield potential will remain the same, but the projected yield level will increase by almost 1 tonne per hectare in large parts of France, northern Italy and areas north of the Alps (Figure 4). Irrigated areas in particular were projected to increasingly contrast with non-irrigated areas in the future climate scenarios with regard to both yield level and yield stability, giving rise to the assumption that further yield increases could be achieved by expanding irrigation, particularly in the Balkan states. This projection, however, would require authoritative scenarios of future irrigation water availability at the regional scale, which is beyond the scope of this study.

It is difficult to predict the economic success of soybean in Europe and the extent to which self-sufficiency goals can be met for two major reasons: First, our simulations show that many regions in northern Europe are likely to become suitable for soybean production. However, whether or not farmers would actually start growing soybean depends on (i) the competitiveness of soybean with current dominant cereals, which are likely to remain high-yielding until the mid-century at least (Hristov et al., 2020), (ii) the agronomic options of including soybean in crop rotations (Reckling et al., 2016) and (iii) the development of the demand for soybean for human consumption, which could generate attractive prices for non-genetically modified soybeans (Klaiss et al., 2020). The second reason for the difficulty in predicting economic success is that soybean is not the only crop that can meet protein demands. Other protein-rich legumes, such as broad beans and peas, may turn out to be a better alternative in the diversified cropping systems of some (northern) countries. Nevertheless, there are two main incentives for growing soybean in Europe, which will facilitate the larger-scale introduction of this crop. First, soybean could be produced to achieve protein self-sufficiency (European_Commission, 2018). According to our simulations, this appears to be within reach in some European regions. However, several further factors require attention beyond those we investigated: (i) irrigation water needs to be available to boost yields to the edge of potential, (ii) inoculation of soybean roots with nitrogen-fixing bacteria (e.g. *Bradyrhizobium*) needs to be improved, especially under cool weather conditions (Halwani et al., 2021; Kühling et al., 2018; Zimmer et al., 2016), (iii) farmers need to have the knowledge and markets to sell crops within their region at attractive prices and (iv) human diets need to change to reduce the demand for soybean-based feed for ruminants. Second, climate change adaptation and low-pesticide strategies promote diversification of the cropping system (Reckling et al., 2022) as an important pillar, and soybean—as a nitrogen-fixing legume—offers a range of environmental benefits that have already increased the crop's appeal.

Simulation of soybean grain yields remains a challenge and requires good field data for calibration (Corrales et al., 2022). In our study, we, therefore, collated data sets from various biophysical conditions and maturity groups to achieve a high accuracy of predictions (Table 2). Kothari et al. (2022) found considerable variability among models in simulating soybean yield responses to increasing temperature and CO_2. Heat stress, however, was not investigated in their study, and it seems that suitable data sets for calibrating heat stress algorithms are lacking, especially for European soybean varieties. The high uncertainty in model responses indicated the limited applicability of individual models for climate change food projections, suggesting the use of an ensemble mean of simulations across models. The ensemble is a useful approach to reduce the high uncertainty in soybean yield simulations associated with individual models and their parametrisation (Kothari et al., 2022; Martre et al., 2015). This approach was, therefore, also applied in our study, with four simulation models that are known for their ability to closely reproduce the effects of water supply, temperature and atmospheric CO_2 concentration of crop growth and yield formation (Table 1). As already indicated by Tao et al. (2018), the AEMs in this study also produced a significantly higher uncertainty when predicting yields compared with the GCMs used for driving AEMs, although all AEMs were calibrated to the same experimental data. In some regions of Europe, the standard deviation of the simulated yields even exceeds the average (e.g. Estonia). One effect of this common calibration can be observed in the simulated yield under irrigation. In this case, all models assume almost optimum growth and, therefore, arrive at a very similar potential yield value, which is due to the same maximum yields to which the models were calibrated. Here, the mean standard deviation of the AEMs is often at its minimum, taking values of less than 1 $t\,ha^{-1}$. At the same time, average yields are highest in the irrigated areas, which is why high values of standard deviations also occur here (e.g. Apulia, Andalusia). It remains to note that, despite adopting a rigorous calibration process using a wide range of maturity groups and sites for this study, the different structure of the individual AEMs (Tao et al., 2018) still makes the choice of one AEM out of many a considerable source of uncertainty, supporting the use of the ensemble (Battisti, Sentelhas, et al., 2017; Martre et al., 2015) as a suitable approach for such analysis and projection.

Compared with data-driven approaches, the use of AEMs to produce future projections of crop growth and yield formation under hypothetical conditions, including future climate, facilitates more detailed process analyses. In this study, we were able to disentangle the climatic effect on the soybean physiology, boosting yields under more favourable temperature and CO_2 regimes, and the effect of

farmers' adaptation to climate change by using better-suited MGs. Our analysis suggests that this adaptation measure is an essential component for achieving higher yields in many regions of Europe, necessary to exploit the full potential that warmer temperatures and higher CO_2 levels are expected to provide in the future.

5 | CONCLUSIONS

We conclude that climate change appears to create a lot more potential for growing soybeans at low risk, rendering possible both larger protein self-sufficiency and the diversification of production systems. Here, the expansion of suitable production area increases this potential much more than the average productivity gain. The models suggest that yield reductions due to drought are overcompensated by the positive CO_2 and temperature effects on photosynthesis in many regions across Europe. It must be noted, however, that the effects of heat on soybean yield potential are yet to be quantified. Taking our estimates for future production as a biophysical potential, the actual extent of any future increase in soybean production will then depend on EU and national priorities and their promotion. Cold spells and wet conditions at harvest will remain major challenges for soybean production in Europe for some time, while drought and heat will become increasingly important. Autumn precipitation is a technical challenge for the harvesting process in northern parts of Europe with short growing periods, but drought and cold tolerance of soybean are already being addressed by plant breeders, especially for regionally adapted cultivars. However, heat tolerance needs to be added to the list of breeding targets, and experimental data to improve the models in this direction is urgently needed. Our simulations demonstrate that the use of currently available later-maturing cultivars promises efficient adaptation to the potential brought about by climate change in many areas of Europe. Irrigation remains the most effective way to increase yields, mitigating both heat and drought stress, but given the water scarcity challenges in Europe (Trnka et al., 2019), this option is not feasible everywhere. Nevertheless, several management options remain underexplored, such as optimised sowing dates (as a drought escape strategy), and double cropping and relay intercropping with cereals in Mediterranean systems. Improving these options will help to further increase the stability and profitability of soybean productivity in Europe.

ACKNOWLEDGEMENT

Open Access funding enabled and organized by Projekt DEAL.

CONFLICT OF INTEREST

All authors declare that they have no conflicts of interest.

DATA AVAILABILITY STATEMENT

The data that support the findings of this study are openly available in the BonaRes Repository at https://doi.org/10.4228/zalf.vjcp-vep3, at the website of the Joint Research Centre at https://esdac.jrc.ec.europa.eu/content/european-soil-database-derived-data and in GitHub (https://github.com/zalf-rpm/soybeanEu-pub).

ORCID

Claas Nendel https://orcid.org/0000-0001-7608-9097
Moritz Reckling https://orcid.org/0000-0002-0689-7686
Philippe Debaeke https://orcid.org/0000-0002-4173-8170
Susanne Schulz https://orcid.org/0000-0001-6216-0593
Michael Berg-Mohnicke https://orcid.org/0000-0001-6687-8295
Julie Constantin https://orcid.org/0000-0001-9647-5374
Stefan Fronzek https://orcid.org/0000-0003-2478-8050
Munir Hoffmann https://orcid.org/0000-0002-9791-5658
Snežana Jakšić https://orcid.org/0000-0002-4387-1434
Kurt-Christian Kersebaum https://orcid.org/0000-0002-3679-8427
Agnieszka Klimek-Kopyra https://orcid.org/0000-0002-7426-2420
Hélène Raynal https://orcid.org/0000-0002-3492-0564
Céline Schoving https://orcid.org/0000-0003-4811-7331
Tommaso Stella https://orcid.org/0000-0002-3018-6585
Rafael Battisti https://orcid.org/0000-0001-5768-4501

REFERENCES

Ainsworth, E. A., Davey, P. A., Bernacchi, C. J., Dermody, O. C., Heaton, E. A., Moore, D. J., Morgan, P. B., Naidu, S. L., Yoo Ra, H. S., Zhu, X. G., Curtis, P. S., & Long, S. P. (2002). A meta-analysis of elevated [CO_2] effects on soybean (*Glycine max*) physiology, growth and yield. *Global Change Biology*, *8*, 695–709.

Allen, R. G., & Wright, J. L. (1997). Translating wind measurements from weather stations to agricultural crops. *Journal of Hydrologic Engineering*, *2*, 26–35.

Alsajri, F. A., Wijewardana, C., Krutz, L. J., Irby, J. T., Golden, B., & Reddy, K. R. (2019). Quantifying and validating soybean seed emergence model as a function of temperature. *American Journal of Plant Sciences*, *10*, 111–124.

Archontoulis, S. V., Miguez, F. E., & Moore, K. J. (2014). A methodology and an optimization tool to calibrate phenology of short-day species included in the APSIM PLANT model: Application to soybean. *Environmental Modelling & Software*, *62*, 465–477.

Avila, A. M. H., Farias, J. R. B., Pinto, H. S., & Pilau, F. G. (2013). Climatic restrictions for maximizing soybean yields. In J. E. Board (Ed.), *A comprehensive survey of international soybean research—Genetics, physiology, agronomy and nitrogen relationships* (pp. 367–375). Rijeka Intech Press.

Battisti, R., Parker, P. S., Sentelhas, P. C., & Nendel, C. (2017). Gauging the sources of uncertainty in soybean yield simulations using the MONICA model. *Agricultural Systems*, *155*, 9–18.

Battisti, R., Sentelhas, P. C., & Boote, K. J. (2017). Inter-comparison of performance of soybean crop simulation models and their ensemble in southern Brazil. *Field Crops Research*, *200*, 28–37.

Boote, K. J., Allen, L. H., Prasad, P. V. V., Baker, J. T., Gesch, R. W., Snyder, A. M., Pan, D., & Thomas, J. M. G. (2005). Elevated temperature and CO_2 impacts on pollination, reproductive growth, and yield of several globally important crops. *Journal of Agricultural Meteorololgy*, *60*, 469–474.

Brisson, N., Gary, C., Justes, E., Roche, R., Mary, B., Ripoche, D., Zimmer, D., Sierra, J., Bertuzzi, P., Burger, P., Bussière, F., Cabidoche, Y. M., Cellier, P., Debaeke, P., Gaudillère, J. P., Hénault, C., Maraux, F.,

Seguin, B., & Sinoquet, H. (2003). An overview of the crop model STICS. *European Journal of Agronomy*, *18*, 309–332.

Carauta, M., Latynskiy, E., Mossinger, J., Gil, J., Libera, A., Hampf, A., Monteiro, L., Siebold, M., & Berger, T. (2018). Can preferential credit programs speed up the adoption of low-carbon agricultural systems in Mato Grosso, Brazil? Results from bioeconomic micro-simulation. *Regional Environmental Change*, *18*, 117–128.

Coleman, K., Whitmore, A. P., Hassall, K. L., Shield, I., Semenov, M. A., Dobermann, A., Bourhis, Y., Eskandary, A., & Milne, A. E. (2021). The potential for soybean to diversify the production of plant-based protein in the UK. *Science of the Total Environment*, *767*, 144903.

Corrales, D. C., Schoving, C., Raynal, H., Debaeke, P., Journet, E. P., & Constantin, J. (2022). A surrogate model based on feature selection techniques and regression learners to improve soybean yield prediction in southern France. *Computers and Electronics in Agriculture*, *192*, 106578.

Denner, M. T., James, A. T., Robertson, M. J., & Fukai, S. (1998). Optimum soybean cultivars for possible expansion area: A modelling approach. *Proceedings of the 10th Australian Soybean Conference*, Brisbane.

Đorđević, V., Balešević Tubić, S., Miladinović, J., & Vasiljević, M. (2021). *Harvesting soybean. Legume hub*. http://www.legumehub.eu

Earthstat. (2000). *Cropland and pasture area in 2000*. http://www.earthstat.org/cropland-pasture-area-2000/

Egli, D. B., & Wardlaw, I. F. (1980). Temperature response of seed growth characteristics of soybeans. *Agronomy Journal*, *72*, 560–564.

Eriksson, D., Kershen, D., Nepomuceno, A., Pogson, B. J., Prieto, H., Purnhagen, K., Smyth, S., Wesseler, J., & Whelan, A. (2019). A comparison of the EU regulatory approach to directed mutagenesis with that of other jurisdictions, consequences for international trade and potential steps forward. *New Phytologist*, *222*, 1673–1684.

European_Commission. (2018). *Report from the commission to the council and the European Parliament: On the development of plant proteins in the European Union*. European Union.

European_Commission. (2019). *Communication from the commission to the European Parliament, the European Council, the Council, the European economic and Social Committee and the Committee of the Regions: The European green deal*. European Union.

Eurostat. (2021). European Commission. http://ec.europa.eu/eurostat

FAOSTAT. (2019). *Statistics Database of the Food and Agriculture Organization of the United Nations*. http://www.fao.org/statistics/databases/en/

Ghafarian, F., Wieland, R., & Nendel, C. (2022). Estimating the evaporative cooling effect of irrigation within and above soybean canopy. *Water*, *14*, 319.

Gibson, L. R., & Mullen, R. E. (1996). Influence of day and night temperature on soybean seed yield. *Crop Science*, *36*, 98–104.

Gray, S. B., Dermody, O., Klein, S. P., Locke, A. M., McGrath, J. M., Paul, R. E., Rosenthal, D. M., Ruiz-Vera, U. M., Siebers, M. H., Strellner, R., Ainsworth, E. A., Bernacchi, C. J., Long, S. P., Ort, D. R., & Leakey, A. D. B. (2016). Intensifying drought eliminates the expected benefits of elevated carbon dioxide for soybean. *Nature Plants*, *2*, 16132.

Guilpart, N., Iizumi, T., & Makowski, D. (2022). Data-driven yield projections suggest large opportunities to improve Europe's soybean self-sufficiency under climate change. *Nature Food*, *3*, 255–265.

Halwani, M., Reckling, M., Egamberdieva, D., Omari, R. A., Bellingrath-Kimura, S. D., Bachinger, J., & Bloch, R. (2021). Soybean nodulation response to cropping interval and inoculation in European cropping systems. *Frontiers in Plant Science*, *12*, 638452.

Hampf, A. C., Stella, T., Berg-Mohnicke, M., Kawohl, T., Kilian, M., & Nendel, C. (2020). Future yields of double-cropping systems in the southern Amazon, Brazil, under climate change and technological development. *Agricultural Systems*, *177*, 102707.

Hatfield, J. L., & Egli, D. B. (1974). Effect of temperature on the rate of soybean hypocotyl elongation and field emergence. *Crop Science*, *14*, 423–426.

Hiederer, R. (2013). *Mapping soil properties for Europe—Spatial representation of soil database attributes*. Publications Office of the European Union.

Hodson, T. O. (2022). Root mean square error (RMSE) or mean absolute error (MAE): When to use them or not. *Geoscientific Model Development*, *15*, 5481–5487.

Holzworth, D. P., Huth, N. I., Devoil, P. G., Zurcher, E. J., Herrmann, N. I., McLean, G., Chenu, K., van Oosterom, E. J., Snow, V., Murphy, C., Moore, A. D., Brown, H., Whish, J. P. M., Verrall, S., Fainges, J., Bell, L. W., Peake, A. S., Poulton, P. L., Hochman, Z., … Keating, B. A. (2014). APSIM—Evolution towards a new generation of agricultural systems simulation. *Environmental Modelling & Software*, *62*, 327–350.

Hristov, J., Toreti, A., Perez Dominguez, I., Dentener, F., Fellmann, T., Elleby, C., Ceglar, A., Fumagalli, D., Niemeyer, S., Cerrani, I., Panarello, L., & Bratu, M. (2020). *Analysis of climate change impacts on EU agriculture by 2050*. Publications Office of the European Union.

Hufnagel, J., Reckling, M., & Ewert, F. (2020). Diverse approaches to crop diversification in agricultural research. A review. *Agronomy for Sustainable Development*, *40*, 14.

Jégo, G., Pattey, E., Bourgeois, G., Morrison, M. J., Drury, C. F., Tremblay, N., & Tremblay, G. (2010). Calibration and performance evaluation of soybean and spring wheat cultivars using the STICS crop model in eastern Canada. *Field Crops Research*, *117*, 183–196.

Jia, H., Jiang, B., Wu, C., Lu, W., Hou, W., Sun, S., Yan, H., & Han, T. (2014). Maturity group classification and maturity locus genotyping of early-maturing soybean varieties from high-latitude cold regions. *PLoS ONE*, *9*, e94139.

Jiang, B., Nan, H., Gao, Y., Tang, L., Yue, Y., Lu, S., Ma, L., Cao, D., Sun, S., Wang, J., Wu, C., Yuan, X., Hou, W., Kong, F., Han, T., & Liu, B. (2014). Allelic combinations of soybean maturity loci E1, E2, E3 and E4 result in diversity of maturity and adaptation to different latitudes. *PLoS ONE*, *9*, e106042.

Karges, K., Bellingrath-Kimura, S. D., Watson, C. A., Stoddard, F. L., Halwani, M., & Reckling, M. (2022). Agro-economic prospects for expanding soybean production beyond its current northerly limit in Europe. *European Journal of Agronomy*, *133*, 126415.

Karlsson, J. O., Parodi, A., Van Zanten, H. H. E., Hansson, P.-A., & Röös, E. (2021). Halting European Union soybean feed imports favours ruminants over pigs and poultry. *Nature Food*, *2*, 38–46.

Kersebaum, K. C. (2007). Modelling nitrogen dynamics in soil-crop systems with HERMES. *Nutrient Cycling in Agroecosystems*, *77*, 39–52.

Klaiss, M., Schmid, N., Betrix, C.-A., Baux, A., Charles, R., & Messmer, M. M. (2020). Organic soybean production in Switzerland. *OCL-Oilseeds and Fats, Crops and Lipids*, *27*, 64.

Kothari, K., Battisti, R., Boote, K. J., Archontoulis, S. V., Confalone, A., Constantin, J., Cuadra, S. V., Debaeke, P., Faye, B., Grant, B., Hoogenboom, G., Jing, Q., Van der Laan, M., da Silva, F. A. M., Marin, F. R., Nehbandani, A., Nendel, C., Purcell, L. C., Qian, B., … Salmeron, M. (2022). Are soybean models ready for climate change food impact assessments? *European Journal of Agronomy*, *135*, 126482.

Koti, S. K., Reddy, V. R., Kakani, G., Zhao, A. D., & Gao, W. (2007). Effects of carbon dioxide, temperature and ultraviolet-B radiation and their interactions on soybean (*Glycine max* L.) growth and development. *Environmental and Experimental Botany*, *60*, 1–10.

Kühling, I., Hüsing, B., Bome, N., & Trautz, D. (2018). Soybeans in high latitudes: Effects of Bradyrhizobium inoculation in Northwest Germany and southern West Siberia. *Organic Agriculture*, *8*, 159–171.

Kurasch, A. K., Han, V., Leiser, W. L., Vollmann, J., Schori, A., Bétrix, C.-A., Mayr, B., Winkler, J., Mechtler, K., Aper, J., Sudaric, A., Pejic, I., Sarcevic, H., Jeanson, P., Balko, C., Signor, M., Miceli, F., Strijk, P., Rietman, H., … Würschum, T. (2017). Identification of mega-environments in Europe and effect of allelic variation at maturity E loci on adaptation of European soybean. *Plant, Cell & Environment*, *40*, 765–778.

Kurosaki, H., & Yumoto, S. (2003). Effects of low temperature and shading during flowering on the yield components in soybeans. *Plant Production Science*, *6*, 17–23.

Lamichhane, J. R., Constantin, J., Schoving, C., Maury, P., Debaeke, P., Aubertot, J.-N., & Dürr, C. (2020). Analysis of soybean germination, emergence, and prediction of a possible northward establishment of the crop under climate change. *European Journal of Agronomy*, *113*, 125972.

Li, Y., Yu, Z., Jin, J., Zhang, Q., Wang, G., Liu, C., Wu, J., Wang, C., & Liu, X. (2018). Impact of elevated CO_2 on seed quality of soybean at the fresh edible and mature stages. *Frontiers in Plant Science*, *9*, 1413.

Malone, R. W., Kersebaum, K. C., Kaspar, T. C., Ma, L., Jaynes, D. B., & Gillette, K. (2017). Winter rye as a cover crop reduces nitrate loss to subsurface drainage as simulated by HERMES. *Agricultural Water Management*, *184*, 156–169.

Mandić, V., Bijelić, Z., Krnjaja, V., Simić, A., Ruzić-Muslić, D., Dragicević, V., & Petricević, V. (2017). The rainfall use efficiency and soybean grain yield under rainfed conditions in Vojvodina. *Biotechnology in Animal Husbandry*, *33*, 475–486.

Martre, P., Wallach, D., Asseng, S., Ewert, F., Jones, J. W., Rötter, R. P., Boote, K. J., Ruane, A. C., Thorburn, P. J., Cammarano, D., Hatfield, J. L., Rosenzweig, C., Aggarwal, P. K., Angulo, C., Basso, B., Bertuzzi, P., Biernath, C., Brisson, N., Challinor, A. J., … Wolf, J. (2015). Multimodel ensembles of wheat growth: Many models are better than one. *Global Change Biology*, *21*, 911–925.

Mirschel, W., & Wenkel, K. O. (2007). Modelling soil-crop interactions with AGROSIM model family. In K. C. Kersebaum, J. M. Hecker, W. Mirschel, & M. Wegehenkel (Eds.), *Modelling water and nutrient dynamics in soil crop systems* (pp. 59–74). Springer.

Nahar, K., Hasanuzzaman, M., & Fujita, M. (2016). Heat stress responses and thermotolerance in soybean. In M. Miransari (Ed.), *Abiotic and biotic stresses in soybean production* (pp. 261–284). Academic Press.

Nendel, C., Berg, M., Kersebaum, K. C., Mirschel, W., Specka, X., Wegehenkel, M., Wenkel, K. O., & Wieland, R. (2011). The MONICA model: Testing predictability for crop growth, soil moisture and nitrogen dynamics. *Ecological Modelling*, *222*, 1614–1625.

Notz, I., Topp, C. F. E., Schuler, J., Alves, S., Amthauer, L., Dauber, J., Haase, T., Hargreaves, P. R., Hennessy, M., Iantcheva, A., Jeanneret, P., Kay, S., Recknagel, J., Rittler, L., Vasiljević, M., Watson, C. A., & Reckling, M. (under revision). Transition to legume-supported farming in Europe through re-designing cropping systems. *Agronomy for Sustainable Development*, in press.

Ohnishi, S., Miyoshi, T., & Shirai, S. (2010). Low temperature stress at different flower developmental stages affects pollen development, pollination, and pod set in soybean. *Environmental and Experimental Botany*, *69*, 56–62.

Ortel, C. C., Roberts, T. L., Hoegenauer, K. A., Purcell, L. C., Slaton, N. A., & Gbur, E. E. (2020). Soybean maturity group and planting date influence grain yield and nitrogen dynamics. *Agrosystems, Geosciences and Environment*, *3*, e20077.

Pannecoucque, J., Goormachtigh, S., Ceusters, N., Bode, S., Boeckx, P., & Roldan-Ruiz, I. (2022). Soybean response and profitability upon inoculation and nitrogen fertilisation in Belgium. *European Journal of Agronomy*, *132*, 126390.

Portmann, F. T., Siebert, S., & Doll, P. (2010). MIRCA2000-global monthly irrigated and rainfed crop areas around the year 2000: A new high-resolution data set for agricultural and hydrological modeling. *Global Biogeochemical Cycles*, *24*, Gb1011.

Puteh, A. B., ThuZar, M., Mondal, M. M. A., Abdullah, N. A. P. B., & Halim, M. R. A. (2013). Soybean [*Glycine max* (L.) Merrill] seed yield response to high temperature stress during reproductive growth stages. *Australian Journal of Crop Science*, *7*, 1472–1479.

Ramankutty, N., Evan, A. T., Monfreda, C., & Foley, J. A. (2008). Farming the planet: 1. Geographic distribution of global agricultural lands in the year 2000. *Global Biogeochemical Cycles*, *22*, GB1003.

Reckling, M., Albertsson, J., Vermue, A., Carlsson, G., Watson, C. A., Justes, E., Bergkvist, G., Jensen, E. S., & Topp, C. F. E. (2022). Diversification improves the performance of cereals in European cropping systems. *Agronomy for Sustainable Development*, *42*, 118.

Reckling, M., Bergkvist, G., Watson, C. A., Stoddard, F. L., & Bachinger, J. (2020). Re-designing organic grain legume cropping systems using systems agronomy. *European Journal of Agronomy*, *112*, 125951.

Reckling, M., Bergkvist, G., Watson, C. A., Stoddard, F. L., Zander, P. M., Walker, R. L., Pristeri, A., Toncea, I., & Bachinger, J. (2016). Trade-offs between economic and environmental impacts of introducing legumes into cropping systems. *Frontiers in Plant Science*, *7*, 669.

Reckling, M., Döring, T. F., Bergkvist, G., Stoddard, F. L., Watson, C. A., Seddig, S., Chmielewski, F.-M., & Bachinger, J. (2018). Grain legume yields are as stable as other spring crops in long-term experiments across northern Europe. *Agronomy for Sustainable Development*, *38*, 63.

Ritter, L., & Bykova, O. (2021). Sowing time for soybean. *Legumes translated practice note*. www.legumestranslated.eu

Robertson, M. J., & Carberry, P. S. (1998). Simulating growth and development of soybean in APSIM. *Proceedings 10th Australian Soybean Conference*, Brisbane.

Ruane, A. C., Goldberg, R., & Chryssanthacopoulos, J. (2015). Climate forcing datasets for agricultural modeling: Merged products for gap-filling and historical climate series estimation. *Agricultural and Forest Meteorology*, *200*, 233–248.

Ruane, A. C., & Mcdermid, S. P. (2017). Selection of a representative subset of global climate models that captures the profile of regional changes for integrated climate impacts assessment. *Earth Perspectives*, *4*, 1.

Schlenker, W., & Roberts, M. J. (2009). Nonlinear temperature effects indicate severe damages to US crop yields under climate change. *Proceedings of the National Academy of Sciences of the United States of America*, *106*, 15594–15598. https://doi.org/10.1073/pnas.0906865106

Schoving, C., Champolivier, L., Maury, P., & Debaeke, P. (2022). Combining multi-environmental trials and crop simulation to understand soybean response to early sowings under contrasting water conditions. *European Journal of Agronomy*, *133*, 126439.

Schoving, C., Stöckle, C. O., Colombet, C., Champolivier, L., Debaeke, P., & Maury, P. (2020). Combining simple phenotyping and photothermal algorithm for the prediction of soybean phenology: Application to a range of common cultivars grown in Europe. *Frontiers in Plant Science*, *10*, 1755.

Serafin-Andrzejewska, M., Helios, W., Jama-Rodzenska, A., Kozak, M., Kotecki, A., & Kuchar, L. (2021). Effect of sowing date on soybean development in South-Western Poland. *Agriculture-Basel*, *11*(5), 413.

Siebert, L., & Tränkner-Benslimane, K. (2020). *Value chain of soybeans in China and Germany. Summarized results of a study conducted by Li Yumei and an analysis of the German market and potential Sino-German cooperation*. Sino-German Agricultural Centre.

Simon-Miquel, G., Reckling, M., Lampurlanés, J., Marquilles, A., & Bonilla, D. (2021). The potential of soybean to diversify highly productive irrigated Mediterranean cropping systems. *LANDSCAPE 2021 – Diversity for Sustainable and Resilient Agriculture*, Online Conference.

Sinclair, T. R., Neumaier, N., Farias, J. R. B., & Nepomuceno, A. L. (2005). Comparison of vegetative development in soybean cultivars for low-latitude environments. *Field Crops Research*, *92*, 53–59.

Soares, J. C., Zimmermann, L., Zendonadi dos Santos, N., Muller, O., Pintado, M., & Vasconcelos, M. W. (2021). Genotypic variation in the response of soybean to elevated CO_2. *Plant-Environment Interactions*, *2*, 263–276.

Staniak, M., Czopek, K., Stępień-Warda, A., Kocira, A., & Przybyś, M. (2021). Cold stress during flowering alters plant structure, yield and seed quality of different soybean genotypes. *Agronomy*, *11*, 2059.

Sun, H., Jia, Z., Cao, D., Jiang, B., Wu, C., Hou, W., & Han, T. (2011). GmFT2a, a soy-bean homolog of flowering locus T, is involved in flowering transition and maintenance. *PLoS ONE*, *6*, e29238.

Tacarindua, C. R. P., Shiraiwa, T., Homma, K., Kumagai, E., & Sameshima, R. (2013). The effects of increased temperature on crop growth and yield of soybean grown in a temperature gradient chamber. *Field Crops Research*, *154*, 74–81.

Tao, F. L., Rötter, R. P., Palosuo, T., Gregorio Hernández Díaz-Ambrona, C., Mínguez, M. I., Semenov, M. A., Kersebaum, K. C., Nendel, C., Specka, X., Hoffmann, H., Ewert, F., Dambreville, A., Martre, P., Rodríguez, L., Ruiz-Ramos, M., Gaiser, T., Höhn, J. G., Salo, T., Ferrise, R., … Schulman, A. H. (2018). Contribution of crop model structure, parameters and climate projections to uncertainty in climate change impact assessments. *Global Change Biology*, *24*, 1291–1307. https://doi.org/10.1111/gcb.14019

Taylor, K. E., Stouffer, R. J., & Meehl, G. A. (2012). An overview of CMIP5 and the experiment design. *Bulletin of the American Meteorological Society*, *93*, 485–498.

Toleikiene, M., Slepetys, J., Sarunaite, L., Lazauskas, S., Deveikyte, I., & Kadziuliene, Z. (2021). Soybean development and productivity in response to organic management above the northern boundary of soybean distribution in Europe. *Agronomy*, *11*, 214.

Trnka, M., Feng, S., Semenov, M. A., Olesen, J. E., Kersebaum, K. C., Rötter, R. P., Semerádová, D., Klem, K., Huang, W., Ruiz-Ramos, M., Hlavinka, P., Meitner, J., Balek, J., Havlík, P., & Büntgen, U. (2019). Mitigation efforts will not fully alleviate the increase in water scarcity occurrence probability in wheat-producing areas. *Science Advances*, *5*, eaau2406.

Tsubokura, Y., Watanabe, S., Xia, Z., Kanamori, H., Yamagata, H., Kaga, A., & Harada, K. (2014). Natural variation in the genes responsible for maturity loci E1, E2, E3 and E4 in soybean. *Annals of Botany*, *113*, 429–441. https://doi.org/10.1093/aob/mct269

US Regional Soybean Laboratory. (1946). *Results of the cooperative uniform soybean test 1945: Part I north central states* (Vol. *131*). US Regional Soybean Laboratory Mimeograph.

US Regional Soybean Laboratory. (1953). *Evaluation of soybean germplasm: A summary of data pertaining to soybean introductions of group I maturity* (Vol. *168*). US Regional Soybean Laboratory Mimeograph.

Wallach, D. P., Martre, P., Liu, B., Asseng, S., Ewert, F., Thorburn, P. J., Ittersum, M., Aggarwal, P. K., Ahmed, M., Basso, B., Biernath, C., Cammarano, D., Challinor, A. J., de Sanctis, G., Dumont, B., Eyshi Rezaei, E., Fereres, E., Fitzgerald, G. J., Gao, Y., … Zhang, Z. (2018). Multimodel ensembles improve predictions of crop–environment–management interactions. *Global Change Biology*, *24*, 5072–5083.

Webber, H., Ewert, F., Olesen, J. E., Müller, C., Fronzek, S., Ruane, A. C., Bourgault, M., Martre, P., Ababaei, B., Bindi, M., Ferrise, R., Finger, R., Fodor, N., Gabaldón-Leal, C., Gaiser, T., Jabloun, M., Kersebaum, K.-C., Lizaso, J. I., Lorite, I. J., … Wallach, D. (2018). Diverging importance of drought stress for maize and winter wheat in Europe. *Nature Communications*, *9*, 4249.

Willett, W., Rockström, J., Loken, B., Springmann, M., Lang, T., Vermeulen, S., Garnett, T., Tilman, D., DeClerck, F., Wood, A., Jonell, M., Clark, M., Gordon, L. J., Fanzo, J., Hawkes, C., Zurayk, R., Rivera, J. A., de Vries, W., Majele Sibanda, L., … Murray, C. J. L. (2019). Food in the Anthropocene: The Lancet Commission on healthy diets from sustainable food systems. *The Lancet*, *393*, 447–492.

Willmott, C. J., Robeson, S. M., & Matsuura, K. (2012). A refined index of model performance. *International Journal of Climatology*, *32*, 2088–2094.

Yamaguchi, N., Yamazaki, H., Ohnishi, S., Suzuki, C., Hagihara, S., Miyoshi, T., & Senda, M. (2014). Method for selection of soybeans tolerant to seed cracking under chilling temperatures. *Breeding Science*, *64*, 103–108.

Yang, W. Y., Wu, T. T., Zhang, X. Y., Song, W. W., Xu, C. L., Sun, S., Hou, W. S., Jiang, B. J., Han, T. F., & Wu, C. X. (2019). Critical photoperiod measurement of soybean genotypes in different maturity groups. *Crop Science*, *59*, 2055–2061.

Żarski, J., Kuśmierek-Tomaszewska, R., Dudek, S., Krokowski, M., & Kledzik, R. (2019). Identifying climatic risk to soybean cultivation in the transitional type of moderate climate in Central Poland. *Journal of Central European Agriculture*, *20*, 143–156.

Zimmer, S., Messmer, M., Haase, T., Piepho, H. P., Mindermann, A., Schulz, H., Habekuß, A., Ordonf, F., Wilbois, P., & Heß, J. (2016). Effects of soybean variety and Bradyrhizobium strains on yield, protein content and biological nitrogen fixation under cool growing conditions in Germany. *European Journal of Agronomy*, *72*, 38–46.

Zipper, S. C., Qiu, J. X., & Kucharik, C. J. (2016). Drought effects on US maize and soybean production: Spatiotemporal patterns and historical changes. *Environmental Research Letters*, *11*, 094021.

SUPPORTING INFORMATION

Additional supporting information can be found online in the Supporting Information section at the end of this article.

How to cite this article: Nendel, C., Reckling, M., Debaeke, P., Schulz, S., Berg-Mohnicke, M., Constantin, J., Fronzek, S., Hoffmann, M., Jakšić, S., Kersebaum, K.-C., Klimek-Kopyra, A., Raynal, H., Schoving, C., Stella, T., & Battisti, R. (2022). Future area expansion outweighs increasing drought risk for soybean in Europe. *Global Change Biology*, *00*, 1–19. https://doi.org/10.1111/gcb.16562